T.C.
SAKARYA UNIVERSITY
INSTITUTE OF SCIENCE AND TECHNOLOGY

NANO SILICON REINFORCED CARBON ANODES FOR HIGH-CAPACITY LITHIUM ION BATTERY: STATE OF CHARGE (SOC) AND BATTERY LIFE TIME TESTING

M.Sc. THESIS

Salman AHMAD

Department	**:**	**NANOSCIENCE AND NANOENGINEERING**
Field of Science	**:**	**NANOSCIENCE AND NANOENGINEERING**
Thesis Supervisor	**:**	**Assoc. Prof. Dr. Tuğrul ÇETİNKAYA**

September 2022

T.C.
SAKARYA UNIVERSITY
INSTITUTE OF SCIENCE AND TECHNOLOGY

NANO SILICON REINFORCED CARBON ANODES FOR HIGH-CAPACITY LITHIUM ION BATTERY: STATE OF CHARGE (SOC) AND BATTERY LIFE TIME TESTING

M.Sc. THESIS

Salman AHMAD

Department : NANOSCIENCE AND NANOENGINEERING

This thesis has been accepted unanimously /with majority of votes by the examination committee on 30/09/2022.

DECLARATION

I declare that all the data in this thesis was obtained by myself in academic rules, all visual and written information and results were presented in accordance with academic and ethical rules, and there is no distortion in the presented data, in case of utilizing other people's works they were refereed properly to scientific norms, the data presented in this thesis has not been used in any other thesis in this university or in any other university.

Salman AHMAD

30.09.2022

ACKNOWLEDGEMENT

Words cannot extend my gratitude to my supervisor Dr. Tuğrul Çetinkaya for his continuous support and help with everything throughout this journey. This also would not have been possible without Dr. Mahmud Tokur, who freely provided his expertise and tutored me with the lab work. I am also thankful to all the people and lab mates for their guidance, especially the concerned team of the SARGEM for providing me with technical support. I am also grateful to Dr. Tariq Kamal for his motivation and moral support.

Lastly, I would be careless in not mentioning my family, particularly my brother, who has always invested in me and stood by me. Their emotional support and belief in me always kept my spirits high throughout my career.

TABLE OF CONTENTS

LIST OF SYMBOLS AND ABBREVIATIONS

LIB	: Lithium-ion battery
Si	: Silicon
MCMB	: Mesocarbon microbeads
EVs	: Electric vehicles
HEVs	: Hybrid electric vehicles
SEI	: Solid electrolyte interface
SOC	: State of charge
CB	: Carbon black
OCP	: Open circuit potential
SEM	: Scanning electron microscopy
EDS	: Energy dispersive spectroscopy
CV	: Cyclic voltammetry
EIS	: Electrochemical impedance spectroscopy
CMC-Na	: Sodium-carboxymethylcellulose
XRD	: X-ray diffraction
DMC	: Dimethyl carbonate
FE-SEM	: Field emission scanning electron microscopy
mAh	: MilliApmere hour
Wt%	: Weight percentage
PVDF	: Polyvinylidene fluoride
°C	: Degree celsius
V	: Volts

LIST OF FIGURES

LIST OF TABLES

SUMMARY

Keywords: Lithium-ion battery, anode, silicon/graphite composite anodes, mesocarbon microbeads, state-of-charge,

The importance of active materials for anodes has gained significant attention in recent times. Carbonaceous materials are typically used as anode candidates in lithium-ion batteries (LIBs), but their low theoretical capacity of 372mAh/g restricts their applications in advanced LIBs. Therefore, Silicon (Si) is considered a prominent alternative anode material for LIBs to replace graphite. Since the theoretical capacity of Si is ten times higher than graphite; however, it suffers from massive mechanical deformations induced during cycling. For this purpose, composites of Si-graphite are proposed for better cycling performance and increased specific capacity. Herein, nano Si powder (<100nm) containing mesocarbon microbeads (MCMB) composites are prepared, and their rate capabilities as anode material for LIBs have been investigated at different current densities. Diverse compositions of the active anode materials (Si and MCMB), carbon black (CB), a binder sodium carboxymethylcellulose (CMC-Na), and distilled water as a solvent have been utilized for the fabrication of anodes, and the fabricated anodes have been morphologically and electrochemically characterized. Moreover, the state-of-charge (SOC) analysis has been evaluated by setting three different upper and lower cut-off voltages.

Our analysis revealed that a composite comprising the lowest Si content (5wt%) exhibited better rate performance and retained a capacity of 455mAh/g after 60 cycles. 15wt% Si showed the worst rate capability performance. Similarly, in theSOCanalysis,a moderate voltage window between 1-0.05V was found optimalon the basis of rate capability results. Voltage window between 1-0.07V lead to quick capacity loss and large surface cracks confirmed in FESEM images. Additionally, in the SOC analysis, 5wt% Si showed the best cycling performance and lost only 10% of its capacity at 1C and 13% at C/2 after 200 cycles between 1-0.05V.

YÜKSEK KAPASİTELİ LİTYUM İYON PİLLER İÇİN NANO SİLİSYUM TAKVİYELİ KARBON ANOTLAR: ŞARJ DURUMU (SoC) VE PİL YAŞAM ÖMÜR TESTİ

ÖZET

Son zamanlarda anotlar için aktif maddelerin önemi büyük ilgi çekinmektedir. Karbonlu malzemeler tipik olarak lityum iyon pillerde (LIB0'ler) anot adayları olarak kullanılır, ancak 372mAh/g'lık düşük teorik kapasiteleri, gelişmiş LIBpiller 'deki uygulamalarını kısıtlar. Silikon (Si), LIB'lerde grafitin yerini alması için önde gelen bir alternatif anot malzemesi olarak kabul edilmektedir. Bunun sebebi, Si'nin teorik kapasitesi grafitten 10 kat daha fazla olmasıdır;ancak, çevrim sırasında büyük hacim değişikliklerinden muzdariptir. Bu amaçla, daha iyi çevrim performansı ve artan özgül kapasite için Si-grafit kompozitleri önerilmektedir. Burada, mezokarbon mikro boncuk (MCMB)kompositi içeren nano silikon tozu (<100nm) hazırlanmış ve lityum iyon pillerin anot malzemesi olarak farklı akım yoğunluklarında oran yetenekleri araştırılmıştır.Aktif anot malzemelerin çeşitli kompozitleri (Si &MCMB), karbon siyahı (CB), bağlayıcı sodyum karboksimetil selülozu (CMC-Na) ve çözücü olarak damıtılmış suyun çeşitli bileşimleri anotların üretimi için kullanıştır, üretilen anotlar elektrokimyasal olarak karakterize edilmiştir. Ayrıca akülerin farklı voltaj pencerelerindeki şarj durumu (SOC) da incelenmiştir.

Analizimiz, en düşük Si (ağırlıkça %5) içeriğine sahip kompozitin daha iyi hız performansı sergilediğini ve 60 çevrim sonrası 455mAh/g'lık kapasiteyi koruduğunu tespit edilmiştir. Benzer şekilde, şarj durumu (SOC) analizinde, hız kapasitesi sonuçları temelinde 1-0.05V arasında bir optimal gerilim penceresi (voltagewindow) bulundu. 1-0.07V arasındaki voltaj penceresi, FESEM görüntülerinden bilindiği gibi hızlı kapasite kaybına ve büyük yüzey çatlaklarına neden olmuştur. Ek olarak, şarj durumu (SOC) analizinde, ağırlıkça %5 Si en iyi çevrim performansını göstermiştir ve 1-0.05V arasında 200 çevrimden sonra 1C'de kapasitesinin sadece %10'unu ve C/2'de %13'ünü kaybetmiştir.

CHAPTER 1. INTRODUCTION

Each day, the world consumes nearly 159,000TWh of energy to meet basic needs, and it is increasing due to the growthin population and industrial development. The contemporary world is making considerable efforts to store energy that could be beneficial for later use. However, this field confronts many challenges because of the unsustainable nature of the non-renewable energy sources and the CO_2 emissions associated with global warming. People around the globe are striving for other environmentally friendly renewable energy sources to minimize CO_2 emissions. Thus, energy from wind and waves, solar radiation, hydropower, etc., has been widely explored. But, due to the unpredictable behavior of these energy sources, proper energy storage and distribution systems are urgently needed. Therefore, batteries are the utmost device, which has demanding applications in almost every field, such as electric vehicles (EVs), solar panels, mobile phones, laptops, and numerous other devices because of their high volumetric and gravimetric energy density [1]. The world has experienced a significant scientific improvement in this field, and its applications are rapidly increasing in the commercial sector.

Rechargeable batteries come in a variety of chemistries, such as nickel-cadmium, lead-acid, and nickel-metal hydride. Among them, lithium-ion batteries (LIBs) are inspiring devices that offer the highest development potential for advanced energy storage of clean energy. However, their improved power density makes them ideal for high-power applications. Also, LIBs are lighter in weight and run at a voltage of approximately 4 V. LIBs comprise 49% of the global battery market, followed by lead acid batteries with 43%. The design capability and performance of LIB for a wide range of applications make its use common in several fields [2]. Further improvement in batteries regardingtheir stability, cycle life, and environmentally friendly limitations are some of the critical challenges for electrochemical scientists.

The most pertinent issues for the electrochemical energy storage industry are enhancing energy and power densities, specific capacity, charging/discharging rate, and life span. In the case of high power needs, further research into developing high-capacity electrode materials is required, and nanomaterials play a critical role in this regard. A simple way to increase the power density is to replace the conventional microparticles with nanoparticles made of electrochemically active materials with a higher specific surface area. During the past few decades, various nanostructured materials have been explored for the fabrication of electrodes [3].Active research work deals with multiple sections of the LIB, such as positive and negative electrodes, electrolytes, electrode-electrolyte interfaces, etc. However, anode is theprimary element in LIBs and affects battery performance.

Carbon compounds are commonly used as negative electrodes in LIBs, with graphitic carbon being the most common. Graphite is more stable in crystalline form, with atoms arranged in a hexagonal fashion. It is a favorable anode candidate because it is economical and chemically stable [4], but its theoretical capacity of 372mAh/g hinders its practical uses in advanced LIBs. Thus, silicon (Si) has replaced graphite as a choice, the 2nd most rich element on earth (about 28%), and offers a theoretical capacity of 3579mAh/g, which is ten times higher than graphite. It has a low discharge voltage of ~ 0.4 volts (V) against Li/Li^+ and is eco-friendly [5]. The Si structure can tend to hold ten times the total number of lithium ions [6]. However, it suffers from structural instability caused by large volume expansion of around 300% to 400% of its original size during lithiation and delithiation. As a result of the repetitive process of intercalation and deintercalation of lithium ions, an inside pressure builds up on Si particles that can damage the surface of the electrode. This fracturing of Si particles is referred to as “pulverization,” resulting in poor cycle life and electrical isolation between the particles and the current collector, due to which Si does not take part in battery capacity, and finally leads to quick capacity loss[7, 8].Another major contributor to anode degradation is the creation of a Solid Electrolyte Interface (SEI), created from the electrolyte decomposition during the first lithiation. Itacts as a blockade between the electrolyte and the electrode. Si is mixed with other elements like carbonaceous materials to solve this dilemma to

develop a composite electrode. Such composites modify Si-based anode materials, which is a recent hot research topic.

The said problems are associated with battery aging mechanisms which occur upon cycling and time. However, according to some recent studies, the behavior of Si-based electrodes changes mostly in a half-cell configuration where Si is cycled against lithium as a counter electrode and can react differently in full lithium-ion cell operation.

1.1. Motivation

The aim of this thesis wasto produce a high-capacity anode material for LIB by mixing a small amount of nano Si powder with a carbon slurry to make a Si-MCMB nanocomposite anode. The Battery Testing Software and Data Analysis (BTSDA) from MTI Corporation has been used to investigate the fabricated coin cells' electrochemical charge/discharge testing. Moreover, cyclic voltammetry (CV) and electrochemical impedance spectroscopy (EIS) techniqueshave also been conducted. The cells are tested at various c-rates [C/10, C/5, C, 2C, and 1C] to see if the incorporation of Si could improve the specific capacity. The morphologies have been analysed through scanning electron microscopy(SEM), and energy dispersive spectroscopy(EDS) before and after the electrochemical testing. Finally, the state-of-charge (SOC) of the batteries has beenexaminedinthree different voltage windows. For high-capacity battery cell technology, novel electrode materials are necessary. The motivation of this work stemmed from learning about the aging phenomenon, which is inevitable in battery cells and eventually causes capacity loss.

1.2. Problem Statement

- LIBs are essential components of renewable energy systems, electric vehicles, smart grids, mobile phones, and laptops. Nevertheless, capacity fade upon battery usage is a major issue and must be scientifically addressed.

- Similarly, even with new developments, the technology of the battery is not flawless, and one fundamental problem still exists, i.e., Battery degradation, which is inevitable.

- A solution is required to guarantee a suitable battery life in all conditions that cannot be achieved without further developments in cell design, usage optimization and a basic understanding of the aging phenomena.

1.3. Thesis Structure

This dissertation hasthe following five chapters.

- Chapter-1, This section includes an overview and importance of LIBs, and elaborates the motivation of work, problem statement, and objective of the research work.

- Chapter-2,This chapter gives a detailed literature review on lithium-ion batteries and recent developments.

- Chapter-3, This chapter describes the research methodology for the preparation of electrodes, such as making slurries, coating on a copper foil, electrode drying, cell assembling, electrochemical measurements, and materials characterization.

- Chapter-4,This chapter explains the electrochemical and physical characterization of the half-cell batteries investigated with different characterization techniques.

- Chapter-5,It is the summary of thesis.

CHAPTER 2. LITERATURE REVIEW

2.1. Background

Environmental pollution, climate change, and an increase in the price of traditional energy sources are the causes of concern around the world. People around the world are turning to alternative energy sources to replace finite fossil fuel sources, having already embraced renewable energy resources like wind energy, solar energy, and wave energy, but at a cost that necessitates storage. Despite the fact that the electricity grid, electromagnetic waves, and chemical energy are all popular energy sources, chemical batteries are feasible energy storage devices. There are numerous advantages to using a battery as a storage device, including portability and the effective conversion of chemical energy into electrical energy without any gaseous emissions [9].

Sony initially manufactured LIBs in 1991, adopting the Asahi firm's research in Japan. LIBs have several features, notably high energy density and no memory effect, and as a result of these characteristics, batteries have rapidly dominated the market. Lithium has the distinction of being the lightest metal element, which results in an increased gravimetric density. It is also the most electropositive metallic element with a potential of -3.04V compared to an ordinary hydrogen electrode, leading to a high energy density electrochemical storage device [10, 11]. $LiCoO_2$ and graphite were utilized in the first generation of LIBs, which were extensively used in power source applications and portable electronic devices such as smartphones and computers [12].

Scientists became more aware of the need for clean energy as time passed, resulting in the development of novel energy storage technologies. To considerably minimize

CO_2emissions in the automobile industry, diesel engines should be supplanted with zero-emission automobiles. Electric vehicles (EVs), hybrid electric vehicles (HEVs), and plug-in electric vehicles all rely heavily on LIBs. Renewable energy resources are expanding across the world; therefore, effective energy storage technologies, such as stand-alone power stations, will play a key role in the future [13]. The amount of electricity generated in a battery can be measured in terms of weight (Wh/kg) or volume (Wh/I), with the cell potential (V) and capacity (Ah.kg) being the determining factors. Table 2.1. presents a comparative study of LIBs with different battery technologies.

Table 2.1.Differentiation and properties of various battery systems [14, 15]

Battery type	Operating Voltage (V)	Energy Density (Wh/kg)	Comments
Lead acid	1.9	30	Generally referred to as a car battery, low energy density
Alkaline	1.5	50-80	Primary device, high capacity for low-power devices
Ni-metal hydride	1.2	60	Memory effect, low energy density
Li-ion	4.0	150	Lighter, high voltage, no memory effect, expensive, high capacity, better charge retention

The type and quantity of active materials decide the maximum amount of energy that can be obtained from the battery. However, only a small portion of the battery's theoretical energy is produced in practice. This is because electrolytes, current collectors, and other non-reactive elements like castings and containers are essential. It is necessary to upgrade LIB technology before it can be used in electric vehicles and larger stationary storage solutions. Commercial reasons encompass lower costs as well as the need for safety. Cyclability, higher energy and power density, and better working cell temperature range are all aspects that must be tackled [11, 16].

2.2. History And Development

In 1800, Alessandro Volta, an Italian physicist, conducted the first systematic research on electrochemistry. He revealed that zinc and copper are able to produce electrical energy through the decomposition of water and generate hydrogen when they are dipped in an acidic electrolyte. It was the first time an electrochemical energy storage device was discovered. Michael Faraday followed the making of rechargeable batteries with liquid electrolytes, particularly lead-acid batteries by Gaston Planté in 1859, nickel-cadmium batteries by Waldemar Jungner in 1899, and nickel-iron batteries by Thomas Edison in 1901, and established some basic electrochemistry laws.

The first idea to build lithium-based rechargeable batteries was initiated in the 1960s, and since then, battery technology has revolutionized. Metallic lithium was initially thought to be an anode because of its high capacity, but it failed due to various safety concerns during cycling, such as dendritic lithium formation, which damages the separator and eventually causes a short circuit [17].

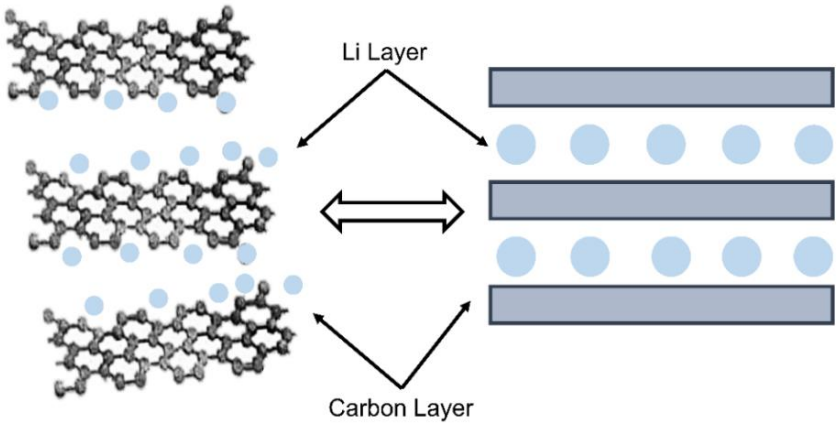

Figure 2.1.Composition of graphite and lithium intercalation [18]

Carbon anodes were later used in commercial battery systems because they were safer than lithium metal anodes. The disclosure of intercalation materials accelerated the development of LIBs. In1970s, Whittingham discovered titanium disulfide (TiS_2) as a productive cathode material intercalating lithium ions. By combining his cathode

and metallic lithium, he was able to create a battery with a potential of more than 2V. Goodenough endeavored to consume $LiCoO_2$ as an intercalating cathode in 1980, with a potential of 4V after coupling it with lithium metal in a battery. In 1985, Yoshino used Goodenough's cathode and integrated it with an intercalating carbon anode. Later in 1986, Rachid Yazami demonstrated the electrochemical characteristics of intercalating lithium in graphite [19].

For the first time in 1991, Sony Corporation commercialized LIB,based on the Yoshino model, which was a major innovation in the technology of LIBs.

Table 2.2. Historical evolution of electrochemical cell

Class	Year	Developer	Name
Primary	1800	Alessandro Volta	Voltaic Pile
	1844	William Robert Grove	Grove Cell
	1888	Carl Gassner	Zinc-Carbon Dry Cell
	1975	Sonyo Electric	Li-Mn Cell
	2004	Panasonic Co.	Oxyride Battery
Secondary	1881	Camille Alphonse Faure	Improved Lead-acid Cell
	Year	Developer	Name
	1899	Waldmar Jungner	Nickel-cadmium Cell
	1901	Thomas Edison	Nickel-iron cell
	1946	Union Carbide Company	Alkaline manganese secondary cell
	1970	Exxon Laboratory	Li-Ti disilfide
	1990	Samsung	Nickel-metal hydride
	1991	Sony Co.	Li-Ion

When Goodenough, Whittingham, and Yoshino were developing their battery systems, they envisaged the future uses of LIBs in which everyone would utilize LIB on a regular basis. Their development during the early 1970s energy crisis, as well as the development of LIBs has dramatically increased the possibility of battery-powered automobiles and renewable-energy-powered electrical networks. Nonetheless, after four decades, batteries are expected to have a significant increase in energy from today's 200–300Wh/kg to 350–450Wh/kg, and possibly 500Wh/kg.

Simultaneously, safety protocols would be strengthened, and prices will continue to fall. Table 2.2. [20, 21] above enumerates the brief historical development of batteries.

2.3. Lithium Ion Battery's Operating Principle

A battery is an electrochemical cell that transforms the stored chemical energy into electrical energy. In other words, a battery is a typical electrochemical instrument that holds electrical energy as chemicals. Batteries are mainly classified as primary and secondary batteries. The primary ones are not rechargeable because of the irreversible chemical reaction inside them, and they are thrown away once utilized. At the same time, secondary batteries are rechargeable and can be used several times. A LIB is generally considered as a secondary battery where energy is stored in the form of chemical energy. It happens as a result of the red-ox process, which involves the use of lithium deposition between the two electrodes (cathode and anode), i.e., during the charging and discharging operations, lithium ions travel back and forth between the positive and negative electrodes. That is why they are also called "rocking-chair" devices [22]. The basic elements of LIB are the anode, cathode, separator, and electrolyte, and several materials are used in their fabrication and characterization.

Lithium is retained in the anode and cathode. Throughout the discharge cycles, the positive electrode (cathode) functions as a reductant by absorbing electrons, and the negative electrode (anode) acts as an oxidant by providing electrons. The two electrodes are separated by a separator placed between them that allows lithium ions to stream freely from the anode to the cathode and vice versa. It also inhibits the battery from short-circuiting. The two electrodes are not in contact with one another, but they areelectrically attached by an electrolyte solution that serves as a carrier of lithiumions.

To further comprehend the whole concept, contemplate $LiCoO_2$, which is frequently seen as the cathode material in rechargeable batteries. When a battery is charging,

lithium ions move from the positive side to the negative side. During this phase, electrons are delivered to the anode from an external source (external voltage).During the discharging phase, the anode forwards the ions to the electrolyte and electrons to the external circuit, where the ions intercalate into the cathode and electrons from the external circuit for charge compensation. The redox reaction occurs as follows:

Positive: $LiMO_2 \rightleftharpoons Li_{1-x}MO_2 + xLi^+ + xe^-$ (2.1)

Negative: $C + xLi^+ + xe^- \rightleftharpoons Li_xC$ (2.2)

Overall: $LiMO_2 + C \rightleftharpoons Li_xC + Li_{1-x}MO_2$ (2.3)

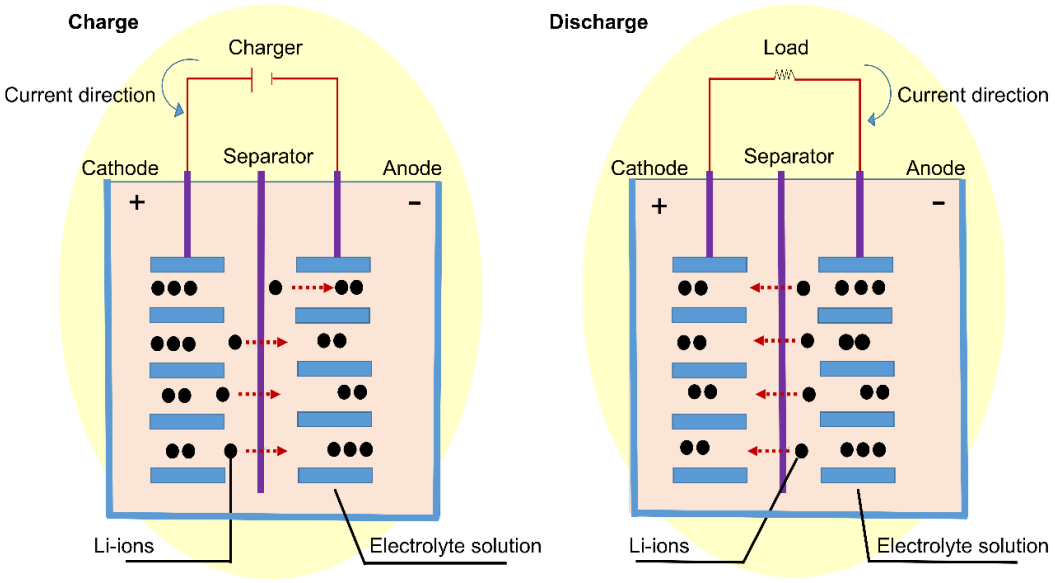

Figure 2.2. Charge discharge mechanism of lithium-ion cell [23].

2.3.1. Anode materials

An anode is generally considered the negative electrode in a primary cell because of the nature of the oxidation reaction. In a secondary cell, the anode is the negative

pole when discharging andthe positive when it is charging. The anode materials used in LIBs have a significant impact on their performance and must have the characteristics of strong ionic conductivity, minimum volume variations, and low specific surface area, usually below $2m^2g^{-1}$ to be safer[24, 25].

Since 1960s, metallic lithium has been used as a fundamental anode candidate in LIBs due to its lowest potential (-3.05V) against the standard hydrogen electrode and having a lower atomic weight of 6.95g/mol. However, there is an unequal deposition of lithium onto the surface of the electrode during the charging conditions. This inhomogeneous lithium plating causes dendrites, which does not allow its further commercialization. This dendrite has a high surface area and diverged lithium metal composition, constantly increasing, which can damage the separator and ultimately lead to some internal short [26]. Therefore, metallic lithium was substituted by carbonaceous materials or lithium intercalation material because of the storage of lithium ions.

Carbon was introduced as an anode material for the first time in 1973. Because of its high carbon content, coke was heavily consumed during the early days of LIB commercialization [27]. On the other hand, MCMB was quickly standardized, with a specific capacity of 300mAh/g and a benign nature [28]. Graphite is chosen as a favorable anode material for LIBs because of its low cost, long life, chemical stability, uniformity, and low operating potential [29]. It is more stable in crystalline form with hexagonally aligned atoms. Its theoretical capacity is 372mAh/g, which is higher than MCMB. However this much capacity is insufficient to meet the requirements of high-energy-density devices when compared to other intercalation materials such as composites (Si/C) [30].

Similar carbon-enriched materials are also readily available. Their electrochemical properties and potential are dependent on the arrangement of carbon atoms. Figure 2.3. depicts the basic structural unit of a hexagonally oriented flattened carbon layer. Fixing these smooth sheets of carbon together creates a multitude of graphite structures. There is a typical hexagonal arrangement of graphite when the ABAB

order is followed, but if ABCABC is put together, it contributes to rhombohedral graphite [31].

Amorphous carbon exists in two types, namely hard carbons, and soft carbons. Both are getting attention in modern applications to deliver very high power and energy density with better safety measurements. Their capacities vary depending on the initial material used and the preparation environment, with hard carbons having a higher capacity than graphite and well current capability. They also have the ability to accumulate more lithium ions than graphite.

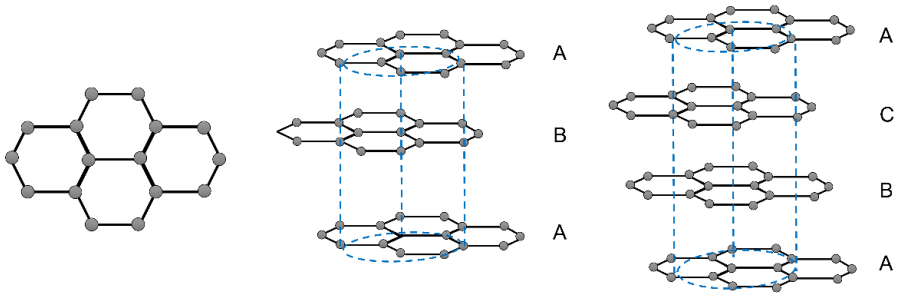

Figure 2.3. Basic Carbon sheet, formation of hexagonal and rhombohedral graphite.

The role of nanostructured carbonaceous materials is important. They possess a large surface area and contain more active locations to store lithium. Plenty of such materials have been manufactured to increase energy and power density. Carbon nanofiber (CNF) is a favorable one with a capacity of almost 450mAhg^{-1} and has revealed a very fast lithium insertion process. One-dimensional candidates such as nanotubes, nanowires, and nanofibers have delivered a tremendous surface-to-volume relation and better surface doings. Graphene, which is a two-dimensional single layer of carbon nanosheet, holds lithium on either of its sides. With its discharge capacity of more than 500mAhg^{-1}, it can accumulate high lithium quantities [32]. The maximum capacity of graphene is 740mAhg^{-1} based on dual-layer adsorption alignment, higher than the layered graphite [33]. In conclusion, carbons with porous structures have been considered the best materials as they have greater surface area. Thus, the morphologies of these nanocarbons decide their electrochemical performance.

Recently, there has been an increasing concern about finding new anode materials for LIBs. For the advancement of LIBs, materials with increased safety, lower cost, higher energy density, and long life are required. [34-37]. Figure 2.4.shows the specific capabilities of some anode materials and illustrates the promising development in theoretical capacity over the state-of-the-art graphite anode material.

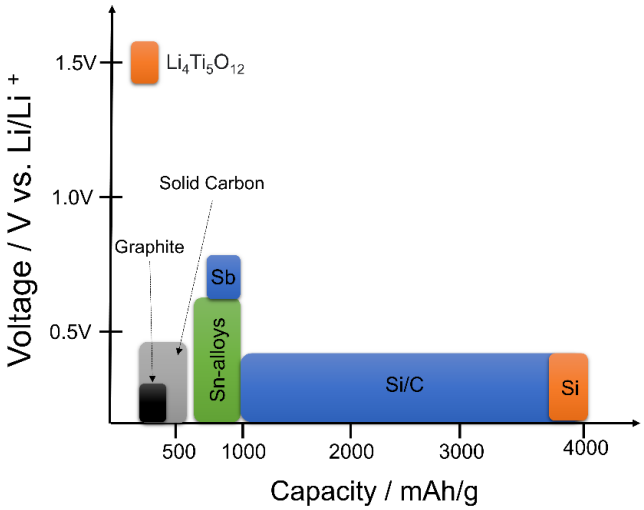

Figure 2.4. Plotted voltage against capacity.

2.3.2. Cathode materials

Over the past two decades, intensified research hasbeen carried out for the improvement of the overall performance of LIBs, and various cathode materials have been discovered. The graphite anodes presently used in LIBs have a theoretical capacity of 372 mAh/g, which is double the theoretical capacity of previously used layered $LiCoO_2$ cathodes and avoids the use of contaminated cobalt.

There are two classes of cathode materials for LIBs. One consists of layered compounds with a dense anion network, the transition metal cations occupy alternating layers between the anion sheets, and lithium ions are injected into the rest of the empty layers. Spinels with transition metal cations arranged in all layers also belong to this group. Therefore, cathodes such as $LiCoO_2$, $LiNiO_2$, $LiNi_{1-x}Co_xO_2$, and $LiMn_2O_4$ belong to this category. These materials have the advantage of higher energy density due to their more compact network, and their topology has easily accessible ion diffusion paths [38, 39]. While the first group of cathode materials has

a more compact network, the second group of cathode materials has more open structures, such as vanadium oxides and transition metal phosphates such as $LiFePO_4$and $LiMnPO_4$ [40]. A summary of the existing cathode materials and their specific capabilities is presented in Figure 2.5.

As mentioned earlier, the first generation of LIBs is made up of $LiCoO_2$ and graphite. $LiCoO_2$ is considered a common cathode material for many practical reasons, such as its preparation and high operational voltage [40]. Li_xCoO_2 has exceptional cycling behavior at room temperature between 1> x> 0.5.

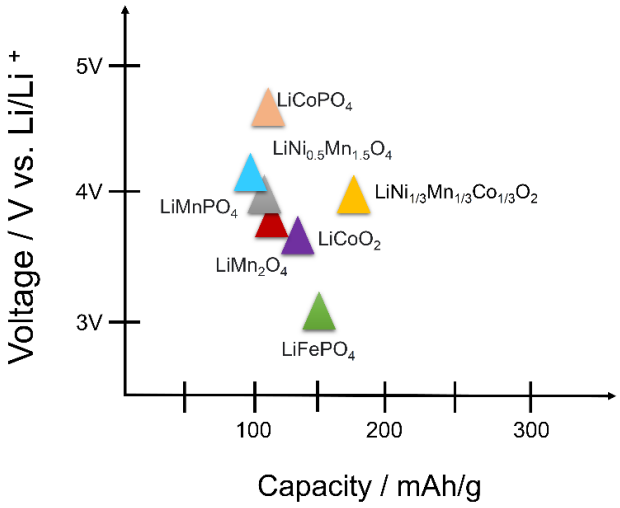

Figure 2.5. Specific capacity of various cathodic materials.

The theoretical capacity of $LiCoO_2$ is 274 mAh/g (Full delithiation), but due to the enormous changes in the anisotropic structure through deep charge, only half of the lithium can be taken out, which corresponds to approximately 50% of its theoretical capacity [14, 41]. The $LiCoO_2$ scheme has been widely explored since its commercialization, and the material is superior regarding cycles and has high physical permanency [42]. On the contrary, $LiCoO_2$ is very costly and toxic andnot easily accessible due to cobalt availability [39]. Hence, alternate cathode materials are required. As shown in Figure 2.5., there are many promising cathode materials, some with advantages of enhanced specific capacities, better cycling response, and energy density, and others withamended safetyfeatures or reduced prices.

Alternatively, the use of $LiMn_2O_4$ as a cathode material is also very interesting because it has lower toxicity and is a plentiful source of material [40], but also because the arrangement of the spinel framework has a flat operating voltage of 3.95-4.1V relative to Li/Li^+gives a theoretical capacity of 148mAh/g [12]. The crystalline structure of the lithium manganese oxide ($LiMn_2O_4$) spinel is given in Figure 2.6., where manganese occupies octahedral positions and lithium mainly dominates tetrahedral locations in the closed compact O^{2-} network [38] that give way to lithiation and delithiation in a three-dimensional network of channels instead of layers like $LiCoO_2$ structure [43].

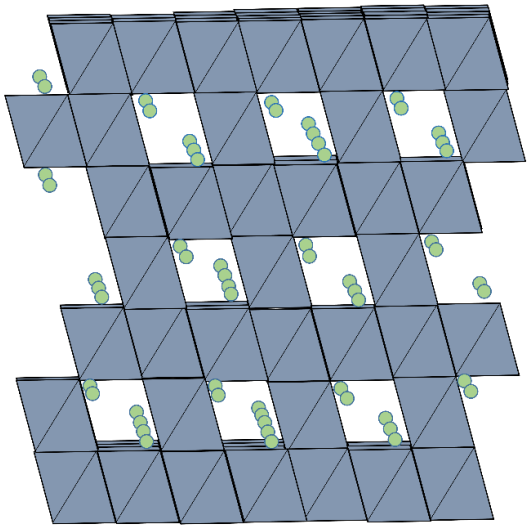

Figure 2.6.Graphical representation of the spinel crystal structure of $LiMn_2O_4$

The discharge of $LiMn_2O_4$ takes place in three stages, two around 4V and the other around 3V, whereby mostly only the 4V plateau is considered [39, 44]. The redox reaction for the charge/discharge process of $LiMn_2O_4$ at 4V is expressed as [45].

$$LiMn_2O_4 \rightleftharpoons Li_{0.5}Mn_2O_4 + 0.5e^- + 0.5Li^+ \quad (2.4)$$

$$Li_{0.5}Mn_2O_4 \rightleftharpoons Mn_2O_4 + 0.5e^- + 0.5Li^+ \quad (2.5)$$

A common problem for spinel $LiMn_2O_4$ is the capacity decay, particularly at high temperatures due to the dissolution of manganese where the concentration of Mn^{3+}

attains its peak value with every discharge. At the surface, the Mn^{3+} may unsymmetrical according to the equation [42].

$$2Mn^{+3} \rightarrow Mn^{+4} + Mn^{2+} \quad (2.6)$$

Another reason is the change in crystallinity, creation of micro-voltages due to the misalliance in the network between two cubic phases developed during cycles, and an increase in oxygen starvation while cycling has been recommended too as a causeof capacity decline [38]. Since Mn^{3+} is often the reason for capacity exhaustion, several efforts have been made to increase the oxidation state of $LiMn_2O_4$ and decrease Mn^{3+} dissolution by doping it with heteroatoms, and several elements have been fabricated to study these properties [38, 40]. Additionally, controlling the particle morphology also decrease capacity loss which reduces the surface area,and the particle size is equally dispersed,improving the electrochemical properties [14, 38, 42].

Many Scientists also give attention to lithium-nickel-manganese oxides ($LiNi_{1-y}MnyO_2$) as a promising replacement for$LiCoO_2$ [46-48]. These composites were first used in 1992 by Dahn et al [47].

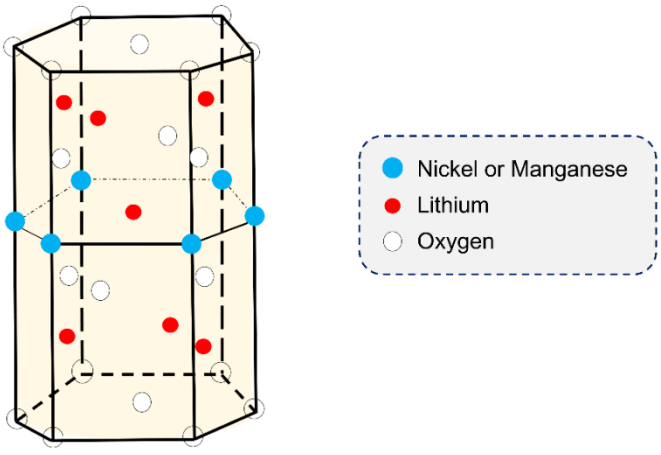

Figure 2.7. Single-cell illustration of LiMnyNi1-yO2, li, Ni, and Mn-filled layers.

The benefit of this material is that it does not contain cobalt, which is a very costly and poisonous substance. The most effective material in this group is $LiNi_{1/2}Mn_{1/2}O_2$. Later on, the authors took up the work of Dahn and revealed solubility of 0.5Mn [48]. They reported on the electrochemical performance of $LiNi_{1/2}Mn_{1/2}O_2$for the first time and exposed that nickel and manganese exist in oxidation states of +2 and +4 instead of +3 and +3, respectively, via XPS and magnetic information. After 25 cycles, the capacity dropped from 150mAh/g to 125mAh/g, and further to 75mAh/g was measured after 50 cycles at 700 ° C.

Another layered metal oxide is $LiMnO_2$ which has the same chemical structure as $LiCoO_2$. It is an inexpensive and environmentally friendly cathode substance than $LiCoO_2$. $LiMnO_2$ permanently changes from Layered into spinel structure during the cycles and quickly loses its capacity [49, 50].

2.3.3. Electrolytes

An electrolyte is a solution of salt and solvents and is the third main constituent of battery after anode and cathode. Liquidelectrolytes in lithium-ion cells work asan ionic conductor to carry lithium ions back and forth between the anode and cathode during the charge-discharge process.

The battery operates at different potential windows for different electrode materials. The working voltage window for LIB ranges from 0-4.5V against Li / Li +, and there is no oxidation nor reduction throughout this range. In order for the LIB to function without deterioration, the electrolyte must remain stable within the same voltage window. Nowadays, electrolytes contain organic liquids such as ethylene-carbonate (EC) and dimethyl-carbonate (DMC). EC and DMC are better solvents for salt due to their high dielectric constants. They also exhibit large and stable electrochemical windows, even below 0–4.5V. But their high vapor pressure can result in a short circuit which limits their applications. In this case, liquid electrolytes are replaced by solid ones to solve this difficulty, which also stops mechanical stress and dendrites' growth [51].The ideal electrolyte would have the following characteristics [14, 48].

- At least 4.5V electrochemical window for lithium-ion cells with high voltage cathodes.
- High electrical conductivity of Li+ over a wide range of temperatures.
- Maintain the electrode/electrolyte interface during the cycle; when the electrode is in use, particles change in volume.
- Chemically and thermally stable.
- Less toxic and cheap.
- Non-flammable and non-explosive.

$LiPF_6$ is significant in keeping Si-based anodes thermally stable in contact with the electrolyte [52]. Electrolytic additives like fluoroethylene-carbonate (FEC) and vinyl-carbonate (VC) have also improved the performance of Si in terms of cycles for such electrodes. [53-55]. Simultaneously, FEC does not let the Si electrode oxidize and decompose. FEC also plays a key role in SEI formation resulting in better cycling performance [47]. VC has already given notable results in terms of coulombic efficiency and in maintaining capacity at such a small concentration of 2% [54].

2.3.4. Separators

Separators are important parts of batteries because they act as a barrier between the anode and the cathode, avoiding any electrical contact between them. They can transfer ions between the two terminals since they are permeable. When selecting a separator, the electrolyte should have enough porosity to allow strong ionic conduction. Microporous LIB separators are the most frequent and widely used seperators [56]. Because the separator is an inactive component in the battery system, scientists have not given much attention to designing and characterizing novel separators [14].

2.3.5. Current collectors

The only purpose of the current collectors is to reversibly transport electrons from the electrodes to the external source. Thus, it is better to select a low resistive collector. There must be enough adhesion between the electrode and the collector so that the electrons can move smoothly between them. Aluminum is a substance that exhibits these features, and it is an excellent candidate for cathode due to its low price and light weight. However, due to (alloying) interactions between lithium and aluminum at moderate potentials, aluminum does not really perform well as a current collector for the negative electrode. As copper does not mix with lithium, it is therefore utilized as the current collector for an anode, despite the fact that it is heavier and even more costly [57, 58].

2.4. Anode Materials

2.4.1. Silicon and graphite

Si is an intriguing substance for the LIB anode for its high theoretical specific capacity of 4200mAh/g at high temperatures and low potentials [51, 59-61]. Because Si as an anode material has several drawbacks, a composite of Si and graphite is a potential material selection for the anode. This combination, in theory, will improve the anode's performance over bare graphite while maintaining graphite's stable reversible cycling characteristics [62, 63].

2.4.2. Graphite as anode material

Graphite is the most common anode material in current commercial LIBs. It has a layered structure, with atoms closely linked to one another inside layers by covalent bonds and moderately linked between layers by van der Waals force. The layered structure of graphite is composed of six carbon atoms that are covalently linked in a hexagonal pattern. Layered patterns are advantageous for electrode materials because they are easy toinsert and remove, allowing ions to intercalate between

layers.Graphite is an excellent anode candidate as it receives charge transfers, suffers from little structural changes upon intercalation, and goes back to its initial form when deintercalated [51]. The biggest limitation of graphite during lithiation is that it is able to hold only one lithium atom for every six carbon atoms in its lattice. As a result, its theoretical specific capacity is just 372 mAh/g.

A thick protective layer is formed on the surface of graphite in the first lithiation cycle, known as the SEI layer. SEI is a stable surface layer composed of organic and inorganic compounds derived from salts, liquids, and contaminants in the electrolyte. It is produced due to lithium redox processes, resulting in an anode capacity loss. SEI affects the anode's safety, power capacity, and cycle life by stopping additional electrolyte breakdown processes on the anode, strengthening the anode's thermomechanical stability, and also stopping future irreversible reactions. The SEI products created on the surface of the electrode are determined by the system's materials [64–66]. The SEI growth on graphite is most prevalent in the 0.8–0.3V potential range [29].

Graphite would experience reduction reactions as the potential is reduced further. The total reduction reaction that takes place once graphite is lithiated while cycling is as follows.

$$C_6 + L^+ + e^- \rightarrow LiC_6 \qquad (2.7)$$

Figure 2.8.depicts the graphite reduction processes and the potentials at which they occur. The reduction reactions are evident as peaks at 0.196 V, 0.11 V, and 0.065 V vs. Li+/Li.

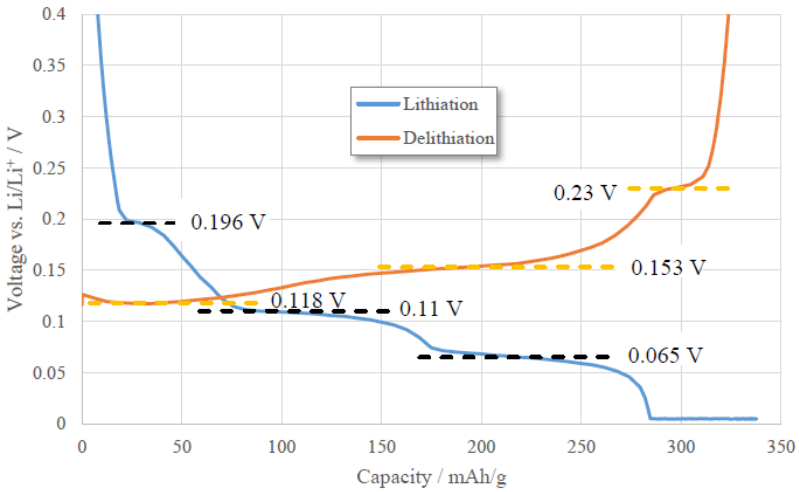

Figure 2.8. A graphite electrode's capacity and voltage curve during the second cycle, with distinct reduction and oxidation potentials upon lithiation and delithiation.

2.4.3. Silicon as anode material

The negative electrode specific capacity,or electrode capacity per unit mass, is an important element in determining a battery's energy density. Si, which has a theoretical capacity of roughly ten times greater than the commonly utilized carbon, has the maximum capacity for lithium-ion batteries. Certainly, the most abundant Li_xSi phase has a theoretical capacity of around 4200mAh/g [68–72]. Despite the fact that increasing the negative electrode's capacity by a factor of ten would only improve the total battery capacity by thirty to forty percent [73]. Si as an anode candidate gained a great attention in recent years [74,75]. Since a Si atom can attach with up to four lithium ions (stoichiometry of$Li_{4.4}Si/Li_{22}Si_5$), whereas it requires six carbon atoms to attach with just one lithium-ion, there is a significant difference in capacitybetween Si and graphite [76,77]. The half-reactions for Si and graphite anodes are given below**.**

$$Li_xSi \leftrightarrow xLi^+ + Si + xe^- \quad (2.8)$$

$$LiC_6 \leftrightarrow Li^+ + 6C + e^- \quad (2.9)$$

2.4.3.1. Complications in silicon anodes

While the performance of Sifor improved LIBs is excellent, there are still several issues with the behavior of Si. These issues stem from themassive volume expansion and contraction upto 400% of its actual size during lithiation and de-lithiation. The value of 400% expansion was discovered by utilizing imaging technologies to validate and record various Li-Si phases as lithium concentration increased [73, 78, 79].SEI development on the surface area of the anode like graphite will result in capacity loss owing to lithium and electrolyte breakdown processes. This is the major problem for Si since it expands during lithiation [59-61]. Because of the irreversible reaction to the creation of the SEI layer, a significant amount of capacity loss is observed, especially during the first cycle. As Si expands and contracts over further cycling, there will be a continuousloss of capacity until the SEI thickness becomes sufficientfor resistance to volume fluctuations.

The mechanical strain and stress that the anode is subjected to during cycling is another problem induced by volume variations in the anode, which causes pulverization of the Si particles, resulting in some particles being separated from the conductive agent bonded to Si. Consequently, it produces empty areas and poor particle interaction, lowering ionic conductivity and causing the capacity to fade since the active material (Si) can no longer be lithiated.One more capacity-limiting flaw of silicon anodes is the lithium diffusion trapping phenomena that happen when lithium ions diffuse gradually upon delithiation of the active material, trapping lithium ions inside the active material and never contributing to additional redox reactions.

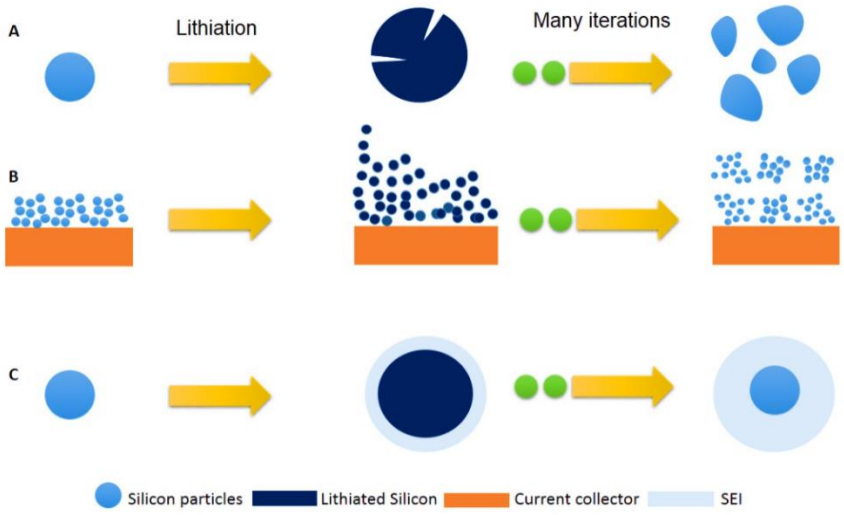

Figure 2.9. Failure mechanisms of Si electrode: (a) material disintegration, (b) Structural and volume variation of the whole Si electrode, and (c) constant SEI development

Using small Si nanoparticles is one of the solutions to avoid pulverization of silicon atoms since they can tolerate mechanical stress better than bigger particles. During the initial cycles, Si undergoes a phase change from crystalline to amorphous Si [61-63, 82] as a result of the reaction process described below.

$$Si(s) + xLi^{+} + xe^{-} \rightarrow Li_{x}Si \qquad (2.10)$$

The starting voltage of this reduction reaction is 0.3–0.4V versus Li/Li+ [59]. Si will remain in amorphous form and will not go back to the pure Si crystalline form after additional cycling. The initial SEI production happens during this process, which has a significant capacity-reducing effect on the battery cell.

During cycling, Si will develop distinct phases based on what cut-off potential it is exposed to. However, in order to reach maximum capacity, it must be cycled to very low potentials, below 50 mV versus Li/Li+ [61, 63, 85]. If Si is cycled to these low potentials, it will change to one of the crystalline stages $Li_{22}Si_5$ or $Li_{15}Si_4$, depending on whether the cycling is done at ambient temperature or at high temperatures.Because of the reduced cycle life induced by this phase change, a lower cut-off voltage beyond 50 mV is recommended to obtain a longer life cycle, though the maximum capacity of Si will not be obtained. The oxidation process takes place

at 0.4V during delithiation. The dissipation of one of the crystalline phases $Li_{22}Si_5$ or $Li_{15}Si_4$, back to the amorphous phase Li_xSi causes this contribution [63]. This reaction stops with additional cycles (no peak), confirming that the silicon remains amorphous.

2.4.4. Silicon/graphite composite anodes

In one reasonable approach to the usage of Si in high-energy LIBs, combining Si with graphite has gained interest and is a viable option for next-generation anodes.

Table 2.3. Comparison of silicon and carbon as anode materials adapted from [86]

Materials	**Silicon**	**Carbon**
Lithiated Phase	$Li_{22}Si_5$	LiC_6
Bulk Density	2.33	2.25
Theoretical gravimetric capacity (mAh/g)	4200	372
Theoretical volumetric capacity (Ah/L)	9781	837
Potential versus Li^+/Li (V)	0.4	0.05
Volume expansion (%)	420	12

Graphite, which acts as a lubricant in Si/graphite blended electrodes, has excellent electrical conductivity and allowscalendaring of the electrode to enhance the density of the composite electrode. Graphite also increases the electrode's preliminary columbic efficiency and stability while reducing volume extension.The electrochemical performances of the Si/graphite composite electrodes are superior to commercial graphitic anodes under normal industrial circumstances for electrode density greater than 1.6 g/cm^3, volumetric capacity greater than 3$mAh/cm^2$and binder quantity 3wt%.

2.4.5. Metal oxide anode materials

Metal oxides have various physical and chemical characteristics as they can offerhigh reversible capacities [28] and can be easily prepared. Hence they are considered as convincing anode materials for rechargeable batteries. In this category, SnO_2 is one of the most significant metal oxides. Lithium is attached to the oxygen in SnO_2 in the first charging cycle, forming Li_2O and pure tin. The mechanism is given below.

$$Sn_2 + 4Li^+ + 4e^- \rightarrow Sn + 2Li_2O \quad (2.11)$$

$$Sn + xLi^+ + xe^- \rightarrow Li_xSn(0 \leq x \leq 4.4) \quad (2.12)$$

As shown in process 2.12, a maximum of 4.4 lithium ions may possibly be added to the Sn-compound, resulting in a theoretical capacity that is considerably higher than graphite. SnO_2 has a theoretical capacity of 781 mAh/g [88], which is double the graphite. The Sn phases formed during the delithiation of the Li-Sn alloy have been seen to consolidate and form a network. H. Li and colleagueshave revealed how the fabrication of $Li_{4:4}Sn$ from stand-alone tin results in a large volume change and poor cycle performance [27]. As a result, it is assumed that the Li_2O matrix produced in mechanism (xx) works as a glue that prevents tin atoms from aggregating [28].

SnO_2 electrodes, on the other hand, experience similar problems with volume variation during lithiation/delithiation. Thus, certain findings are useful for addressing the irreversible capacity declines. Several material compositionshave been explored in this regard, including porous SnO_2 nanostructures, SnO_2nanocomposites, nanostructured SnO_2 thin films,and hollow core-shell mesospheres. Volume variations may be reduced in a porous structure because the pores work as a structural buffer for big volume changes, and the reversible capacity could be greatly improved. Nanostructures such as nanowires and nanotubes follow

the same concept. The increase in the surface area could help to attenuate the volume fluctuations.

The composite materials that combine the benefits of both carbon and SnO_2 are described in [37]. Carbon works as a barrier that avoids aggregation between SnO_2 atoms in SnO_2/carbon nanocomposites by giving a cushioning region in which SnO_2 and Sn atoms could undergo volume variation without being collapsed.

2.5. Aging Phenomena

The most difficult and important task in a battery is to figure out how it ages and degrades. Several elements from the surroundings or usage mode play a role in determining distinct aging effects, making such processes complex. Thus, the capacity loss and resistance rise are not affected by the same factors. As a result, understanding battery aging is very challenging and is, therefore, a recent hot topic in battery research. How it happens and how it affects various battery elements are explained below.

2.5.1. Electrochemical aging

It is the chemical composition of the battery's electrolyte where aging begins. Aging phenomena is different for positive and negative electrodes [89, 90]. The causes of aging mechanisms could be chemical or mechanical, which are significantly influenced by the composition of the electrodes. Aging causes deterioration of the cell components [91], which can result in structural transformation, changes in the chemical composition of the electrolyte, or loss of the active material due to material suspension in the electrolyte, such as manganese [90]. Therefore, electrode deterioration is the primary cause of aging.

2.5.2. Types of aging

The two types of battery aging are calendar aging and cycle aging. In either case,the battery gets old, and it ages with charge-discharge cycles as well as with time, even if not used.

2.5.2.1. Aging with time

The irreversible loss of capacity during storage is referred to as calendar aging; or in other words, it is the deterioration when the battery is not used (stationary conditions) [92, 93], and the rate of self-discharge varies greatly depending on storage conditions. As a result, depending on these circumstances, reactions that take place within the battery could be expedited or decelerated [94].

The storage temperature is a major factor in calendar aging and self-discharge [95]. Supplementary processes like corrosion are accelerated at high temperatures, and loss of lithium is more significant than at mild temperatures, resulting in capacity drop [96, 97]. Low temperatures help to restrict the progression of these processes, but they also cause difficulties because material distribution is lost and the battery chemistry is changed [98].

The SOC levels during storage are another key factor in calendar examinations [99]. Cells do not get age in the same way at the same temperature but with varying SOC. This shows that when the SOC is high, the battery degrades faster [100]. SOC is defined as the percentage of ions present on the electrodes. This indicates an uncertain potential at the interface of electrode/electrolyte for high SOC.

The majority of calendar studies discover SOC in relation to temperature storage conditions. Both these parameters have a direct effect on the calendar aging of the battery. Additionally, capacity decline and resistance increase are not proportional with time, indicating that aging behavior is greatly influenced by time.

2.5.2.2. Aging with cycles

Whenever the battery is charged or discharged, it experiences cycle aging. This is a direct result of the battery's charge level, consumption mode, relative humidity, and present applications. As a result, several factors contribute to such aging. All of the aforementioned features have an influence on calendar aging and are involved in investigations of cycle aging, too, as the aforementioned aging processes occur regardless of the battery utilization.Exothermic reactions are common when batteries are in use [101, 102], and these reactions may accelerate due to elevated temperatures, causing battery aging.It is, nevertheless, necessary to consider the impacts of extremely low temperatures [103].

Besides these parameters, the fundamentals that affect cycle aging are determined by the battery usage type. The change in state-of-charge (ΔSOC) during cycles is commonly reported in the literature. This is an essential consideration when evaluating the quantity of charge occupied (resp.provided) to the battery upon discharging (resp. charge) [104]. The charge/discharge potential throughout the life of a lithium-ion battery is another variable affecting its aging and the operation of the user mode. So, the aging process speeds up with a high charging voltage [105].

2.5.3. Impact on anode

Graphite, silicon, carbon, or titanate account for most anodes [106]. The graphite material used is critical in the aging and safety concerns of the battery [90]. The creation of the SEI layer on the electrode/electrolyte contact with time is the major aging effect on graphite electrodes which is spontaneously formed during the initial charge. It protects the anode from corrosion and the electrolyte from being reduced [107]. The SEI does not remain steady because lithium-ion batteries work under stress outside of the electrolyte's electrochemical steadiness range [108]. Consequently, SEI grows with time, resulting in frequent loss of lithium ions and electrolyte disintegration [109].Furthermore, it has been stated that the major cause

of aging in storage conditions is the loss of accessible lithium due to side reactions at the graphite anode [110].

SEI is also accessible to lithium ions as well as more charged (anion, electrons) or unbiased (liquid) components [89, 111]. As a result of this, the liquid reacts with the graphite following diffusion through the SEI, causing graphite to exfoliate [112] and releasing gas that can rupture the SEI, allowing it to grow [107].The active surface of the electrode diminishes with time, increasing the electrode's resistance. All of these effects occur at the SEI and are given in Figure.10. [89]. This can happen in both the usage and storage conditions of the battery.

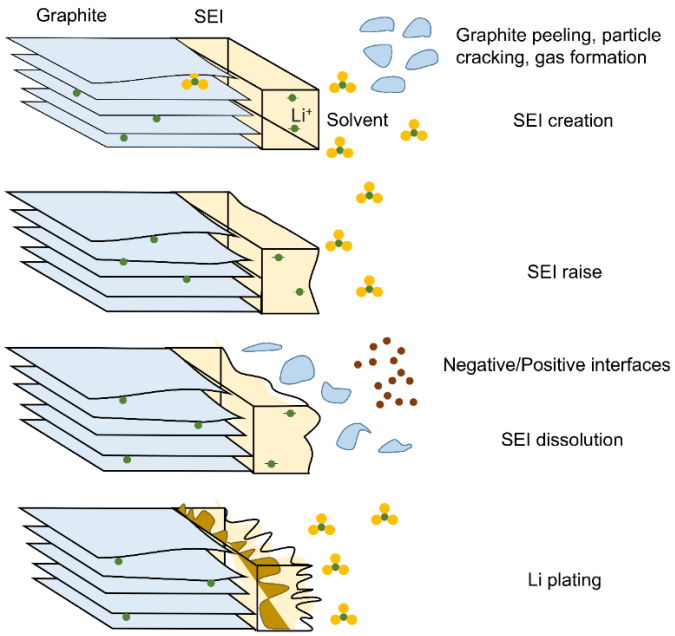

Figure 2.10. Depiction of aging effects on anode: capacity decline and SEI promotion.

Because the potential difference between the electrode surfaces and electrolyte is noteworthy, SOC>80% should promote these processes [113]. Unfortunate situations, such as elevated temperature, overcharging or fault conditions can also speed up the process [114]. Hence, at higher temperatures, the SEI can liquefy, forming lithium compounds with low permeability against lithium ions, raising the negative electrode resistance [115].

2.5.4. Impact on cathode

From positive electrode investigations, it was revealed that the physical structure of the positive electrode does not change at all stages of the battery use,which indicates the vital role of the negative electrode in the battery's aging process [116, 104].Nevertheless, based on the material used, the positive electrode undergoes minor changes over time [117]. Owing to excessive volts on this side, there is also an SEI formation on the electrode/electrolyte interface,which is harder to identify [118, 119]. To summarize, wear of active material, electrolyte worsening, electrolyte ionization, development of SEI, and interactivities between cathode material absorbed inside the electrolyte and anode are the main effects seen on an old positive electrode [120].

Such impacts are not mutually exclusive, and their interrelation varies depending on the positive electrode material chosen [121]. In the case of the negative, assertions strongly rely on temperature and SOC.

CHAPTER 3. EXPERIMENTAL AND METHODOLOGY

Research methodology and experimental procedures are discussed in this section.Materials were prepared, morphologically and electrochemically characterized in the laboratory facility. Details of electrochemical testings and cell assembly are also presented in this chapter.

3.1. Experimental Setup And Materials Used

The following materials are used for the preparation of anodes:

Active materials nano Si powder (<100nm) and mesocarbon micro beads (MCMB, Model: TB-17, from MTI corporation), a binder CMC-Na (Sigma-Aldrich, Co, avg Mw~90,000), conductive agent carbon black (Timcal graphite and carbon super P: emoji: conductive carbon black) and distilled water as a solvent. The anode setup is given in Figure 3.1.

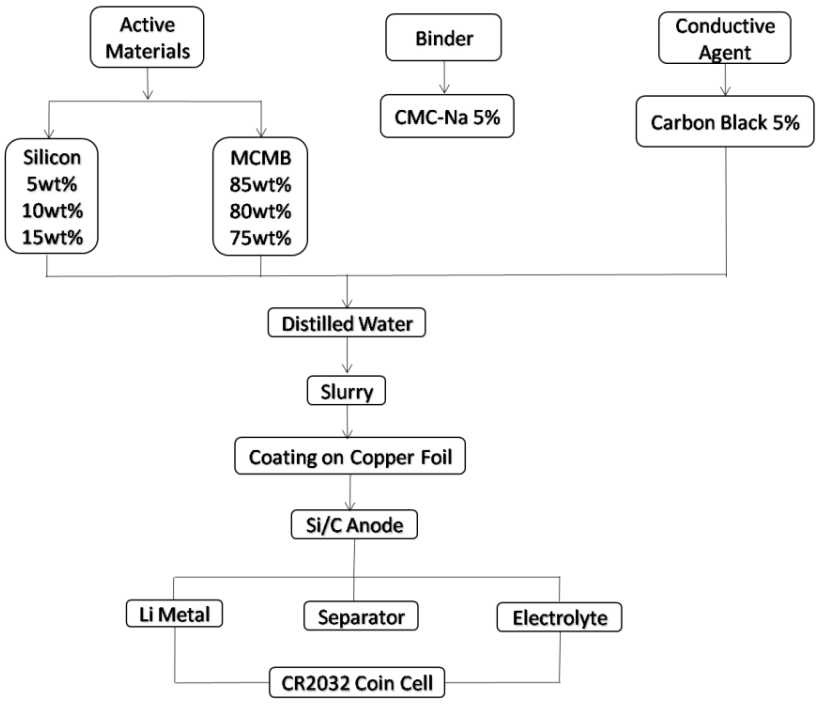

Figure 3.1. Components used in anode

To carefully evaluate various electrode slurries and the performance of the anode, the active material quantity was changed except for the CB and the binder, which were kept constant at 5wt% of the total amount of the material, as shown in Table 3.1.

Table 3.1. Active materials variations in anodes

Anodes	Silicon / (wt%)	MCMB / (wt%)	CB/ (wt%)	Binder/ (wt%)	Mass loading / (mg)	Thickness/ (μm)
Sample 1	5	85	5	5	2.66	30
Sample 2	10	80	5	5	2.75	32
Sample 3	15	75	5	5	2.75	34
Sample 4	0	90	5	5	3.7	32

3.2. Preparation of Electrodes

3.2.1. Materials preparation

Firstly, MCMB was baked for 24 hours in an inert gas oven at 250 °C, while other materials were dried overnight at 100 °C. Most electrode materials are in powder form before being applied to the electrodes. In a standard procedure, this active

material is blended with some amount of a conductive agent. Three samples of Si-MCMB composite electrodes were prepared. The amount of Si was varied as 5wt% for sample 1, 10wt% for sample 2, and 15wt% for sample 3. For comparison, 90wt% of the total amount of active material was used to make bare MCMB electrode (sample 4).

In the beginning, CMC-Na was dissolved in 1200 mg of water to prepare a 5wt% solution and stirred well at 250 rpm for a few hours. CB and CMC-Na were kept at a set value of 5% of the total amount of the solid material. All the samples were thencarefully scaled to prepare a dry slurry. The dry slurry ofthe composite electrodes was mixed well via mechanical alloying for 30-40 minutes to obtain a homogenous mixture of each component. Afterward, the mixture was slowly added to the already prepared CMC-Na binder solution in a small beaker and stirred well for 2 hours at a constant stirrer speed of 250 rpm until all the solids were equally dispersed.

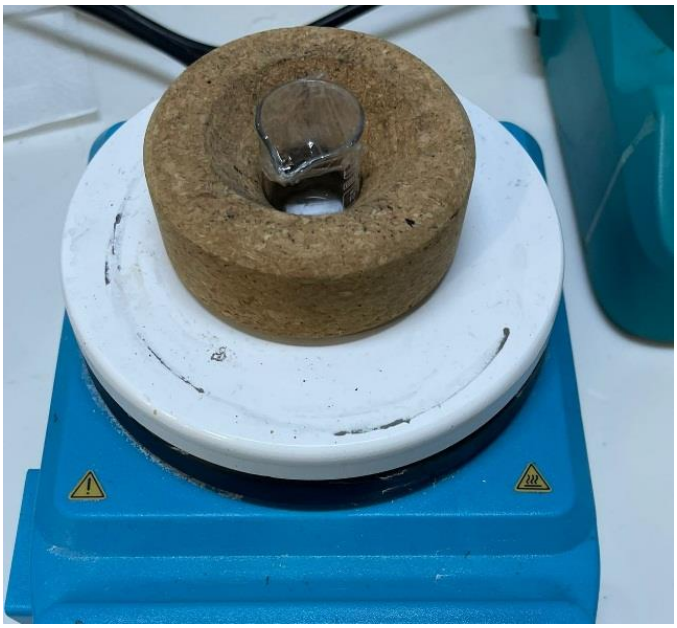

Figure 3.2. Prepared slurry

3.2.2. Coating on a doctor blade

For powdered anode materials, doctor-blading was employed, turning the powder into a slurry and doctor-bladed over a 9 µm thick copper foil. This technique allows

the creation of thin films with precise thicknesses (50 and 100 microns for all samples in this study). Coated slurry and electrode discs are shown in Figure 3.3. below.

Figure 3.3. Pasted slurry on a copper foil and electrode discs

A sharp blade was set at a predetermined gap from the coating surface. The slurry was then poured in front of the blade and pushed linearly over the copper foil, forming a thin wet film behind it. After coating, the foils were dried in an oven for 24 hours at 80 °C. The excellent slurry viscosity and coating conditions made a uniform coating with no cracks. Finally, electrode discs were punched outwith a diameter of 14 mm.

3.2.3. Mass calculations

Weighing each electrode at least five times gave the mass loading for each electrode composition. The mass was calculated by taking the average of the mass difference for each electrode. Simultaneously, the mass of the 9μm thickcopper foil was also measured separately. The final mass loading is determined by subtracting the mass of the copper foil from the average mass of the whole electrode. The mass loading calculations were made after the electrodes were dried in the oven overnight at 80 °C.

3.2.4. Thickness of electrodes

The thickness of the electrodes was measured by randomly evaluating the thickness of the coating on the copper foil at seven different spots and discarding the highest and lowest numbers to eliminate spontaneous thickness inaccuracies. The thickness was computed as a mean of the remaining five measurements. The thickness of the copper foil was subtracted before calculating the electrode's thickness.

3.2.5. Fabrication of half-cell batteries

Before assembling the half-cell batteries, the electrode discs were kept inside the glove box for 24 hours at 120 °C to ensure they were thoroughly dried. For the fabrication of coincells, stainless steel CR2032 cells were assembled in the glove box, filled with argon with less than 0.1ppmO_2 and H_2O. The electrode discs were placed copper-foil down into the bottom case of the coin cell.Lithium iron phosphate ($LiPF_6$) electrolyte with 4:3:3 EC/DMC/DEC was applied,followed by an 18mm Celgard separatorto avoid any short circuit and ensure the electrode was centrally placed. A few more drops of electrolyte were applied to thoroughly soak the separator and the electrode. A lithium metal foil is used as a counter electrodeand carefully cleaned to remove the impurities and put inside the can—followed by two stainless steel spacers and a spring, filling up any extra space inside the cell and confirming that all pieces are in excellent contact. Finally, the closet cap was put over the casing, and the cells were sealed in a crimping machine.

Figure 3.4. Argon filledGlove Box

3.3. Characterization of Electrodes

Field emission scanning electron microscopy (FESEM), energy-dispersive spectroscopy (EDS),and X-Ray diffraction (XRD) are the practical characterization techniques to conduct a comprehensive study of morphologies, chemical compositions, and phase changes of the produced electrodes, respectively.

3.3.1. Scanning electron microscopy (SEM) and energy dispersive spectroscopy (EDS)

SEM is a kind of microscopy that uses a focused stream of electrons to make high-resolution images of material. When electrons collide with atoms in a sample, they produce a variety of signals that reveal details about the surface characteristics and composition of the sample. To create a picture, the electron beam is scanned in a rectangular scan pattern, and its position is coupled with the incoming signal.

FEI (Quanta FEG 450, WV: 15kv, WD: 10.1mm, mode: SE, USA) has beenused to examine the morphology and particle distribution of the electrodes. The measurements are taken at various magnifications to get a good image of the surface features. EDS mapping is performed to see aclear image ofthe homogeneous

composition of the active material particles and their distribution on the surface of the electrode. Both characterization techniques are used for fresh as well as cycled anodes.

3.3.2. X-Ray diffraction (XRD)

XRD is a scientific technique to investigate the crystalline phase variations during the cycling of the battery materials.

3.3.3. Electrochemical characterization

The galvanostatic charge-discharge testing, cyclic voltammetry (CV), and electrochemical impedance spectroscopy (EIS) tests are performed to electrochemically analyze the properties of the fabricated anodes.

3.3.3.1. Galvanostatic charge discharge

Battery Testing Software and Data Analysis (BTSDA, MTI Corporation) is used to galvanostatically charge and discharge the assembled CR2032 coin cells and assess the cycling behavior at a constant current in a standard voltage range for the Si-MCMB composite and bare graphite. The charge/discharge capacities were obtainedunder the standard voltage window between 1.5-0.02V with the testing equipment shown in Figure 3.5.

Figure 3.5. MTI battery testing system for coin cells

3.3.3.2. Cyclic voltammetry (CV)

Potentiostat/Galvanostat/ZRA from GAMRY instruments is used to record CV measurements at a scan speed of 0.3 mV/sec. CV is an electrochemical technique applied to verify the current generation in a cell when the voltage at the working electrode is ramped linearly with time in a predetermined potential range. The same types of cells are used in this analysis as for the rate capability tests.

3.3.3.3. Electrochemical impedance spectroscopy (EIS)

EIS treatments of the half cell batteries consisting of lithium foil as a counter electrode are performed at room temperature with Potentiostat/Galvanostat/ZRA from GAMRY instruments in the frequency range 100 kHz to 10 MHz and signal

amplitude of 20mV. EIS is also an analyzing technique that is used to examinethe reaction mechanism of the electrochemical process. The rate-determining step can be revealed by the frequency response shown by the EIS test because various reaction steps will dominate at particular frequencies. The difference in resistance is investigated by observing the current response. The produced impedance Nyquist curve of the cell consists of a compressed semicircle in the high-frequency range, which represents the resistance of the SEI layer and the charge-transfer resistance (R_{ct}), and the sloping line in the low-frequency region corresponds to the diffusion of lithium ions.

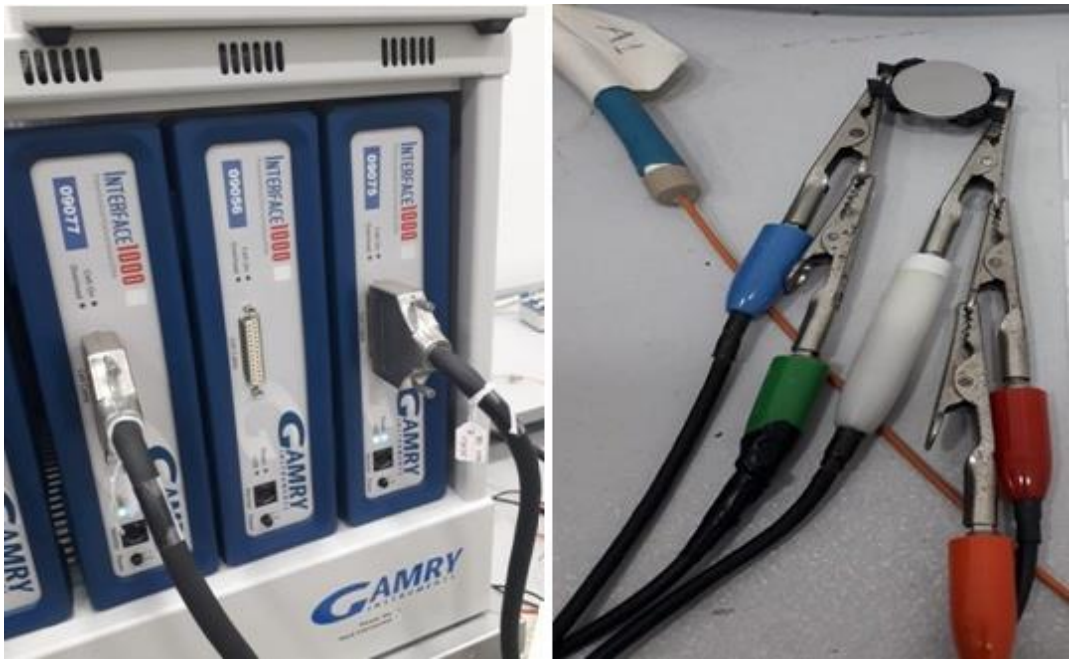

Figure 3.6. Gamry instrument

CHAPTER 4. RESULTS AND DISCUSSION

Nano particles are preferred over micro particles as electrode materials in LIBs due to their shorter diffusion routes for lithium-ion mobility, increased surface area,and superior mechanical capabilities. The small diffusion lengths improve the battery's rate capability and power density, while the increased surface area enhances the interfacial contact between the electrode and electrolyte, resulting in greater rate capability and a long lifecycle. The size of Si powders used in this work is <100nm.

4.1. Structural Characterization

SEM analysis was performed for some of the electrodes to examine the morphology and verify the homogenous distribution of the components inthe electrodes. SEM is an electron microscopy method that produces a magnified image of an object with an electron beam, which is calledthe electron probe and defines the instrument's resolution. It produces a picture of the sample by detecting either of two types of electron emissions from the sample; secondary and backscattered electrons.EDS is a built-in function in the SEM instrument, which uses emitted X-rays to map the chemical composition of the analyzed material [122].

A total of eight samples were characterized before and after the electrochemical testing in the FESEM, including SEM imaging and EDS mapping.

Figure 4.1. below representsthe spherical surface structure of the fresh MCMB electrode. This micrograph reveals that the particle dimensions are in the range of 30–50nm, with several larger particles up to 54nm in width. There is also equal distribution of CB (the small quantity) throughout the surface,as observed in the

literature [123]. The darker black spots on the surface is the binder (CMC-Na). The dark color of the binder in the image is due to its poor conductivity.

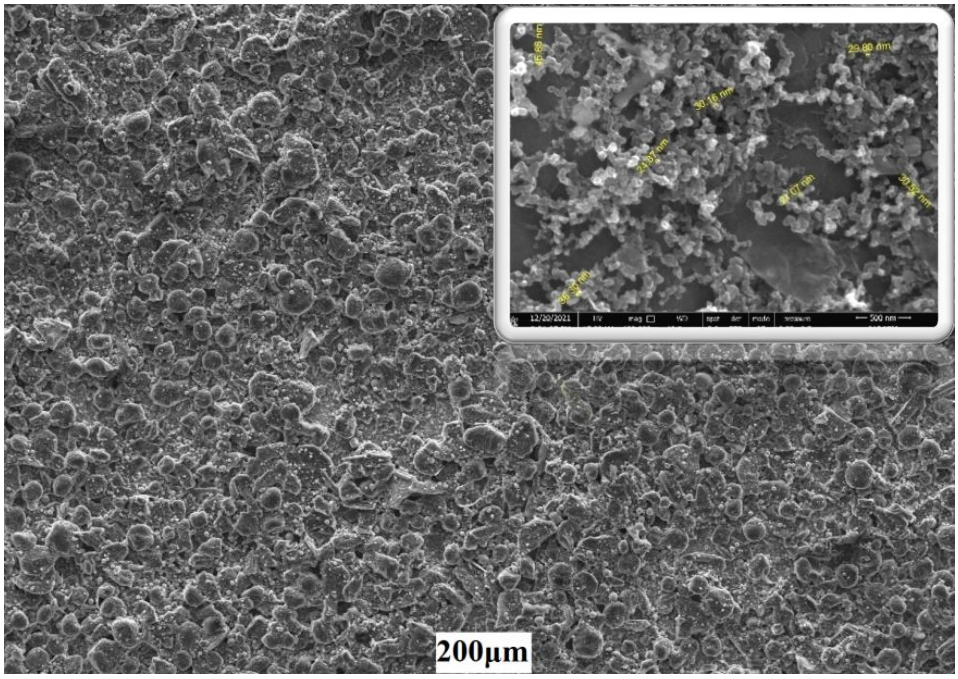

Figure 4.1. SEM image of the fresh MCMB electrode

Figure 4.2. below discloses the morphologies at two different magnifications and particle dispersion on the surfaces of the composite electrodes comprising5wt%, 10wt%, and 15 wt% Si (the percentage is the total active material quantity, and the remainder is MCMB graphite). The tiny shinier particles represent Si, and the larger darkish ones are graphite. As observed, both the Si and graphite particles are uniformly dispersed in all the three composite electrodes. This is critical because it increases the electrochemical and mechanical capability of the electrode [124].The Si enlargement does not stress the neighboring elements when such particle distribution is uniform. The average particle diameters are between 40-70 nm, 50-100 nm, and 30-80 nm for 5%Si/MCMB, 10%Si/MCMB, and 15%Si/MCMB composites, respectively. The CB particles are also homogeneously spread throughout the surface, exactly as they are for the bare MCMB. EDS mapping further confirmed the distribution of each element on the surface of electrodes, as shown in Figure 4.3.

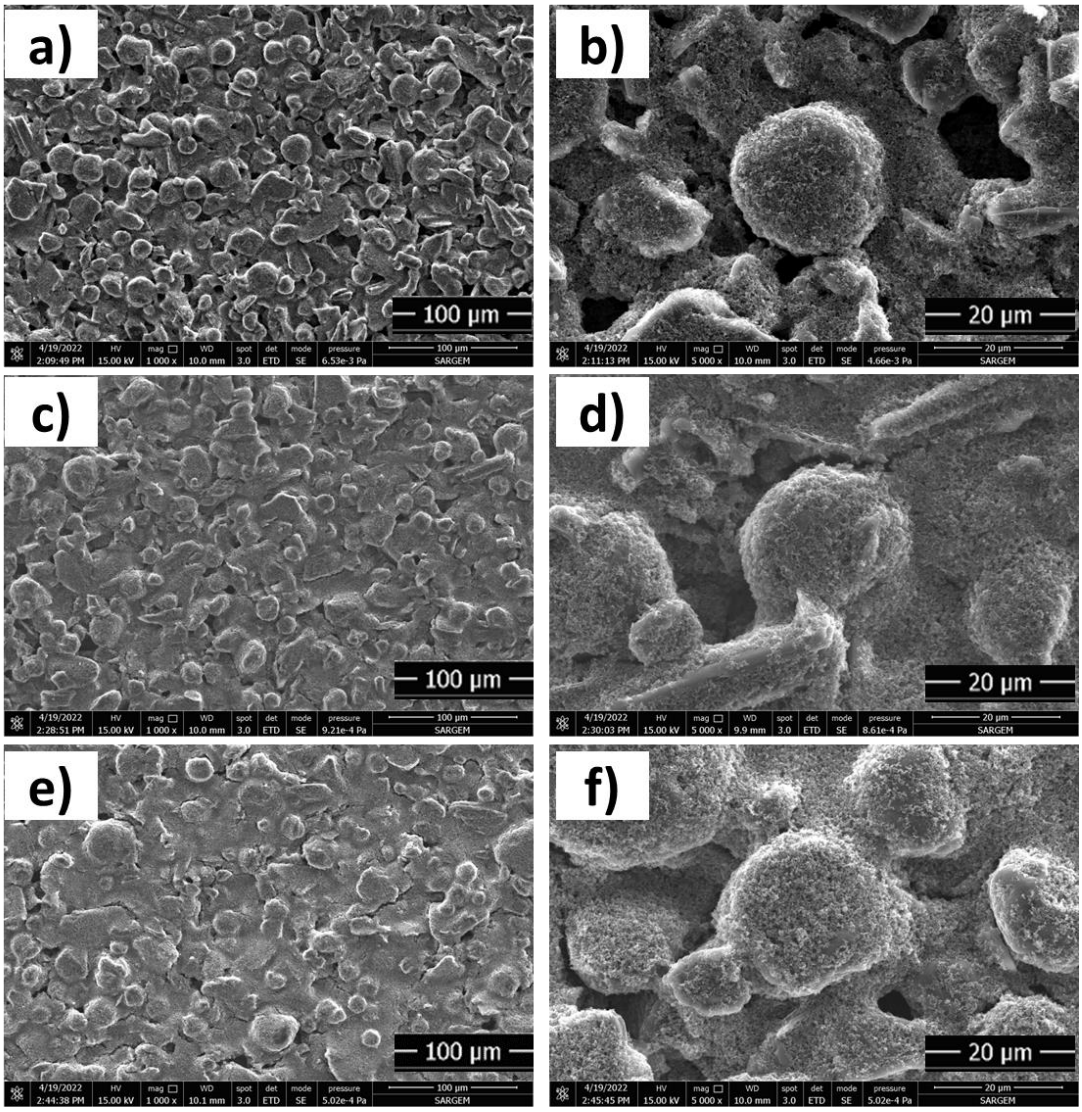

Figure 4.2. SEM micrographs of fresh composite electrodes. (a) and (b) 5% Si/MCMB, (c) and (d) 10% Si/MCMB, (e) and (f) 15% Si/MCMB

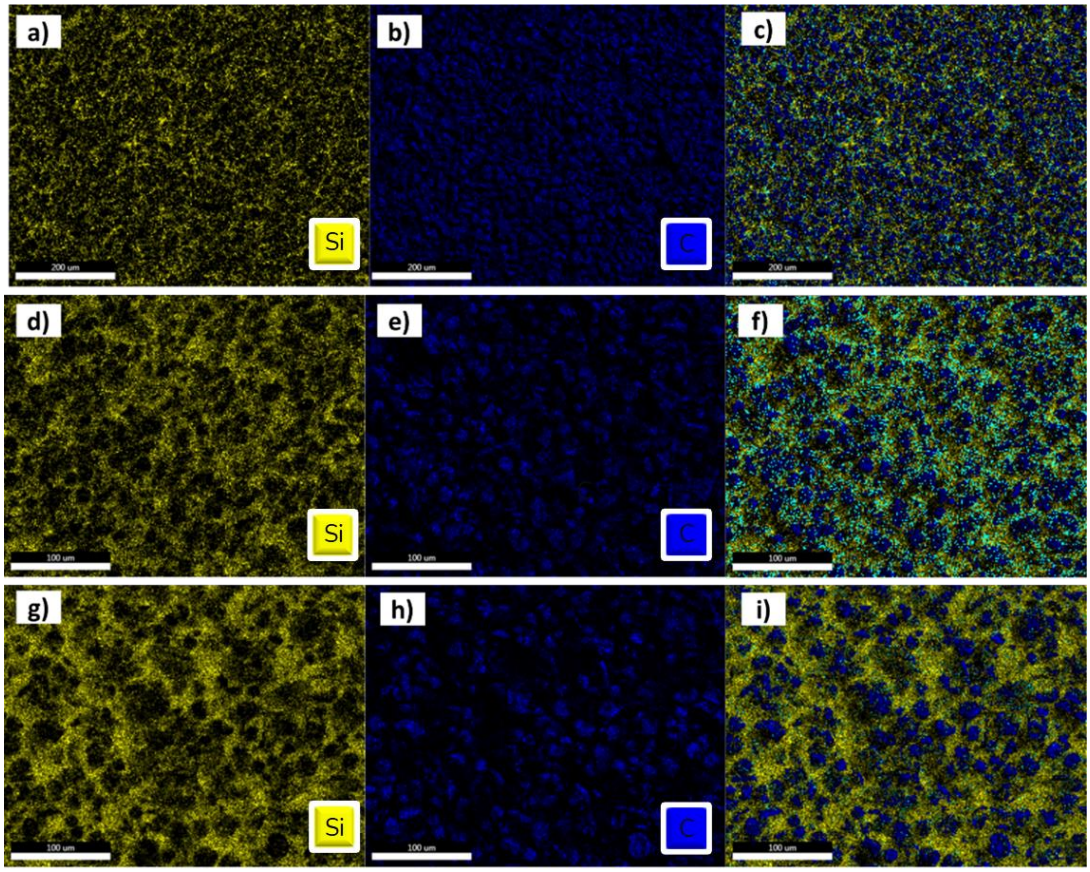

Figure 4.3. EDS mapping of composite electrodes. Yellow is Si and blue is MCMB. (a), (b) and (c) 5% Si/MCMB, (d), (e) and (f) 10% Si/MCMB, (g), (h) and (i) 15% Si/MCMB

EDS mapping was also performed for the composite electrodes to check the composition of each component and to confirm how homogenously the particles are distributed on the electrode surface.Figure 4.3. illustrates high-resolution results where the yellow ones are Si while the blue parts are carbon particles. The picture validates the SEM results that the active material is equally spaced throughout the electrode surface. Furthermore, EDS mapping shows the successful incorporation of Si, especially in the 5wt% sample.

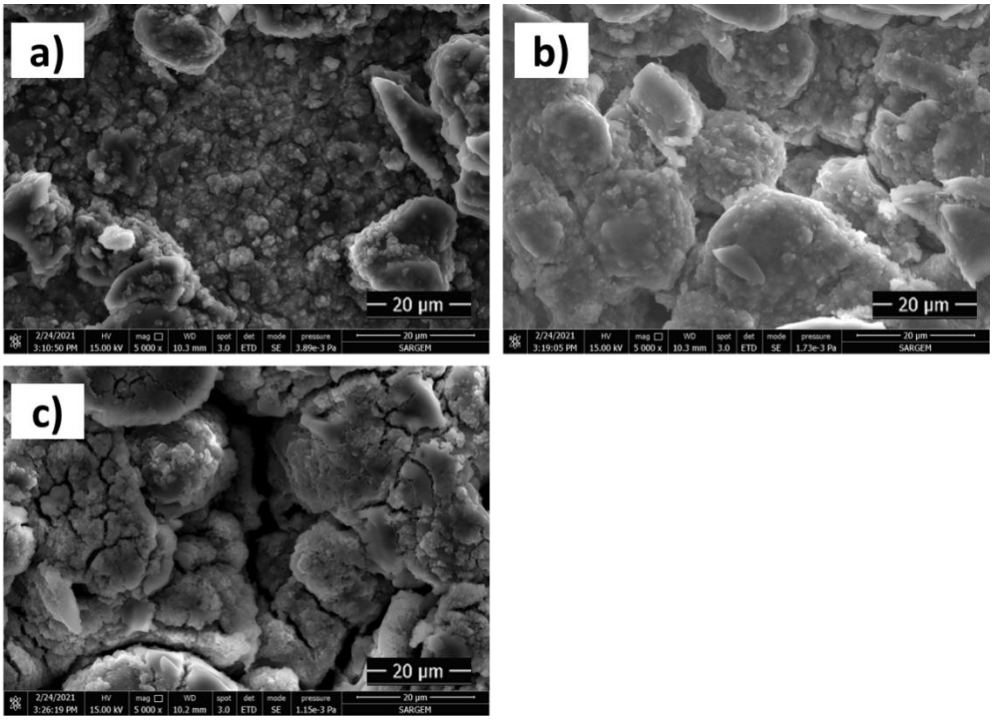

Figure 4.4. Surface textures of cycled electrodes. (a) 5% Si/MCMB, (b)10% Si/MCMB, (c) 15% Si/MCMB

Figure 4.4. above shows that after the electrochemical treatments, the particles experienced large volume expansions in their surface structures, especially in the higher amount of Si content. Moreover, in figure 4.4b, c, cracks can be clearly seen, which is common in Si-based anodes. These newly exposed areas on the electrode surfaces encourage the SEI layer's formation and lead to quick capacity decay. On the other hand, interfacial cracks also promote large surface areas, which contribute to the transportation of lithiumions.

The XRD patterns for the produced anodes are also collected to investigate the phase identification. The patterns of the prepared anodes are presented in Figure 4.5.

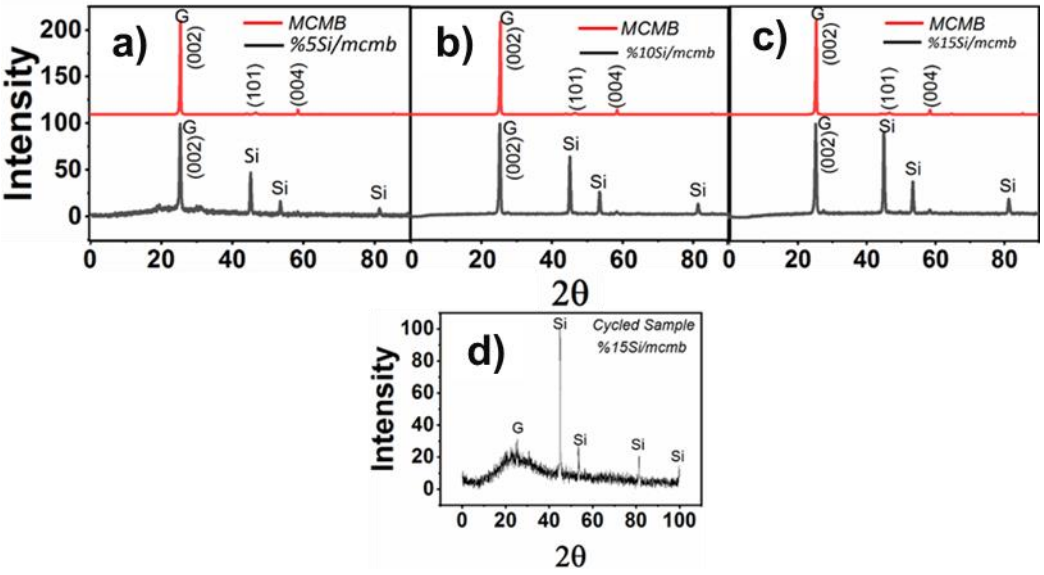

Figure 4.5. XRD Patterns of MCMB and Si/MCMB composites.

The peaks are located at 2θ = 28.4°. 47.3°, 56.1°, 69.1°, and 82° in all the three composites correspond to (111), (220), (311), (400), and (422) planes, respectively. These results match with [125] and illustrate the well-preserved crystalline arrangement after blended with MCMB. For comparison, the XRD pattern of the bare MCMB electrode is also collected. The major XRD peak is located at 2θ =26.50° representing its crystal structure [126]. The full width at half maximum (FWHM) of (002) major peak of MCMB was calculated as 0.283. The presence of graphite peaks around 20-30 and 50-60 in the Si-MCMB composite suggests the contribution of graphite in the chemical reaction. The low intensities of Si (111) and Si (422) in the composite electrodes confirm the nanometer size of the Si. No copper peaks were observed in Si-MCMB composites.

4.2. Electrochemical Characterization

Generally, LIBs, particularly Si-based electrode materials, have a high capacity to fade during initial cycles.For the creation of the SEI layer on the surface of electrodes, it is recommended to perform one or two conditioning cycles (anode pre-lithiation) of the investigated electrode at a low c-rate (C/20 and below) to a low cut-off voltage (down to 0.02 V) before the electrochemical treatment begins. [127, 128].In this thesis, all electrode samples were activated at C/20 (discharge),however,

this step has not been considered in the electrochemical testing. In this discussion, it is worth mentioning that the specific capacity refers to the discharge capacity that has been measured.

A flowchart of the charge-discharge cycling is given in Figure 4.6., where one single discharge (lithiation) cycle was performed at 0.05C under the voltage window of 1.5-0.02V.

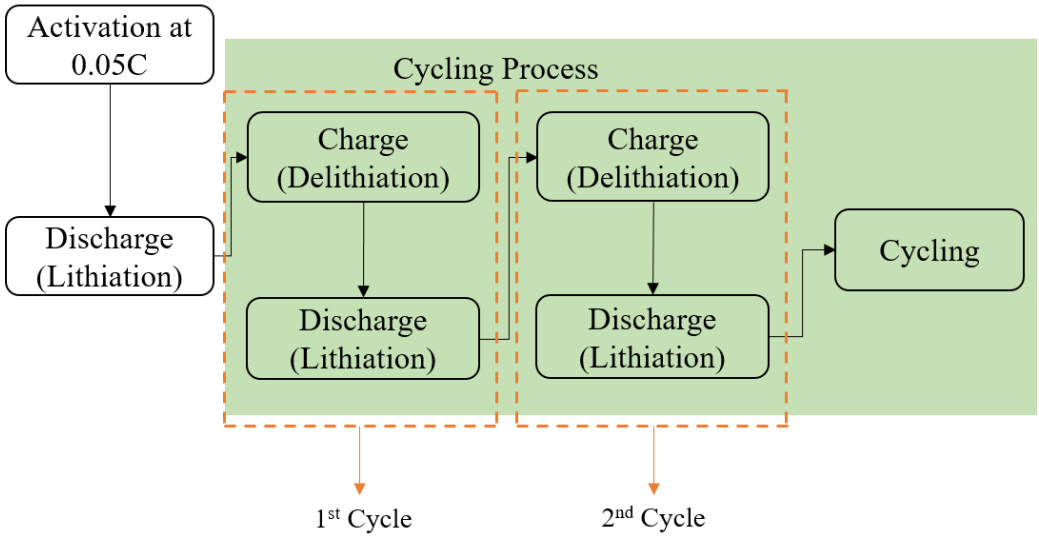

Figure 4.6. Flowchart of charge-discharge cycling

4.2.1. Charge discharge performance of MCMB electrode

All electrode samples were tested for 10 cycles at various c-rates (C/10, C/5, C/2, 1C and 2C).To have a reference for comparison, a bare MCMB graphite electrode with the composition of 90wt% MCMB, 5wt% binder, and 5wt% CB as a conductive agent and a mass loading of 3.7mg was cycled. Results are presented in Figure 4.7.

The rate test for pure MCMB electrode was performed at C/10, C/5, C/2, 1C, 2C, and C/10 again. The electrode was cycled for 10 cycles at each current rate. Figure 4.7 presents the specific discharge capacity of the MCMB electrode. It clearly shows that the MCMB cell has outstanding and stable cycling performance with a capacity of 335.73mAh/g and retained its capacity after 60 cycles. At C/5, the electrode lost its

capacity but showed stable behavior. After increasing the current rate, the capacity loss is huge, which indicates the incomplete transfer of lithium ions from the electrode. At 2C, lithium dendrites may be formed on the counter electrode; however, it stabilizes again at C/10 and reaches the same value as the current reversal can destroy the dendrites' bonds. This evidence shows that MCMB electrodes have poor cycling performance under high cycling conditions.

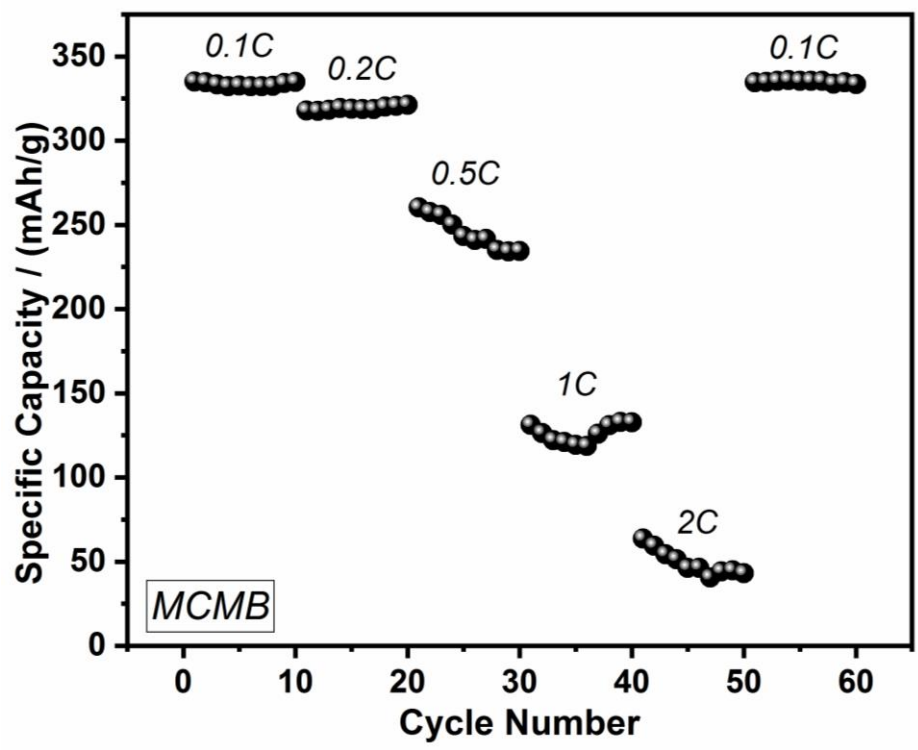

Figure 4.7. Specific capacity of graphite electrode at different current densities

4.2.2. Charge discharge performance of the composite electrodes

A decrease in capacity at high currents can be associated with lithium-ion diffusion theory.Theoretical capacities of the composite anodes were calculated to 532mAh/g for the electrode containing 5wt% Si content, 692.7mAh/g with 10wt% Si content, and 853.05mAh/g for the electrode containing 15wt% Si. All current rates in the electrochemical analysis are based on these capacities. As the electrochemical tests are carried out at room temperature, the possible Si phase could be $Li_{15}Si_4$, with a theoreticalcapacity of 3579mAh/g [129]. The rate performances of the anodes are given in Figure 4.8.

Figure 4.8. shows the rate capability of the composite electrodes and pure MCMB electrode, cycled under 1.5-0.02V.

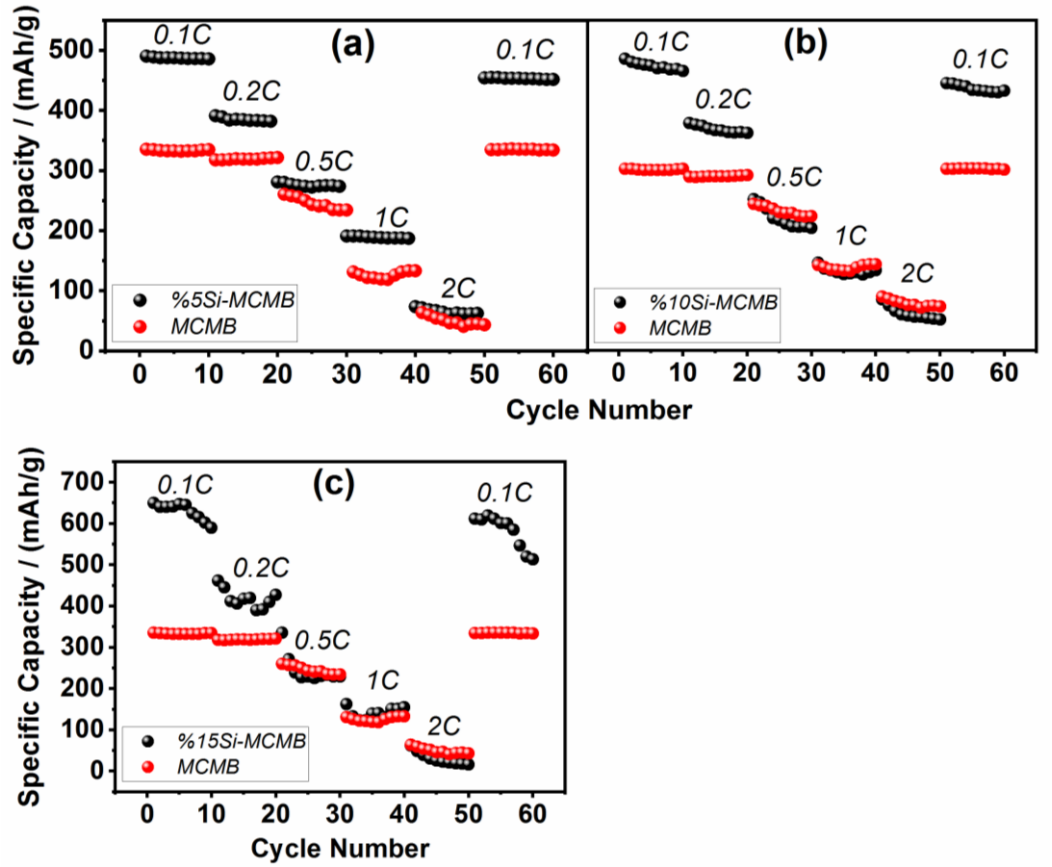

Figure 4.8. Rate performance of composite electrodes vs. MCMB at different current densities

All electrodes were cycled for 10 cycles at each current density. The figure shows that the electrode with a 5wt%Si amount showed the most stable performance and maintained a capacity of 453mAh/g over 60 cycles. At the same time, there is a capacity loss in the initial cycles, particularly in the sample containing the highest Si content (15%). This behavior is due to the creation of the SEI layer on the active material surface and contributed to massive volume changes during cycling [130]. Suppose the electrode is not fully activated through conditioning cycling, in that casethe pulverization of Si particles and the creation of SEI continue for subsequent cycles and can hinder the cell's performance.

It is also remarkable that at higher current densities (1C and higher), the composites containing 10wt% and 15wt% Si content showed very poor capacity performance compared to the bare MCMB electrode,and the capacities have fallen below the pure MCMB electrode. This indicates that the Si particles in the composites no longer remained active in the reaction because of the pulverization and the creation of the SEI layer. These results strongly agree with the SEM analysis that 15w% Si experienced mechanical deformation.

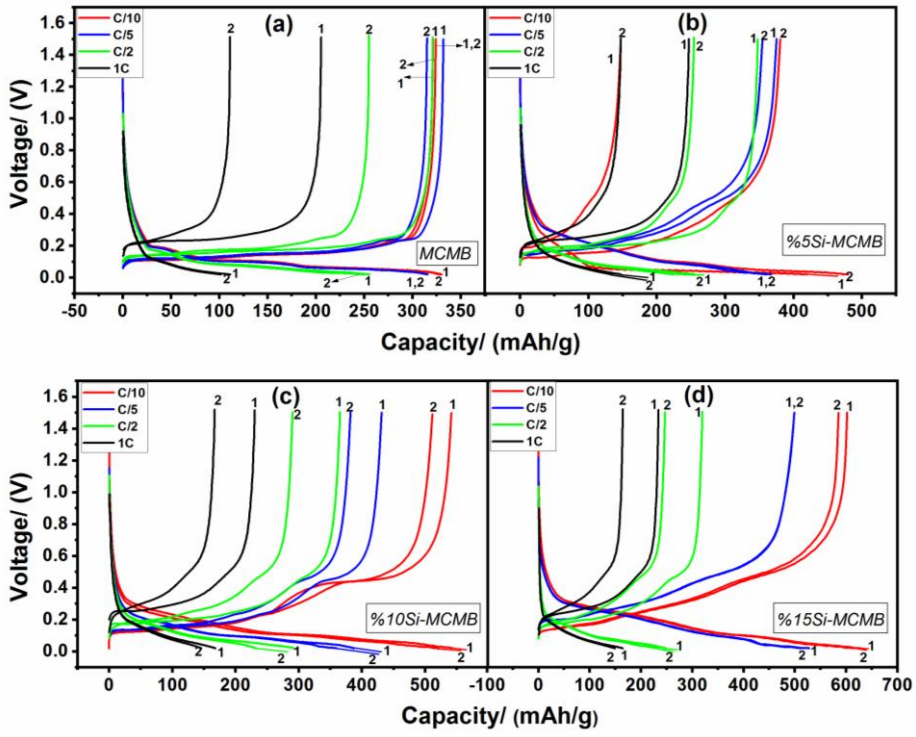

Figure 4.9. Voltage profiles for the 1st and 2nd cycle of the MCMB and composite anodes.

In Figure 4.9., voltage vs. capacity curves profiles of the first two cycles of all the samples, including MCMBare presented.The average charging and discharging voltage profiles for MCMB graphite are around 0.06 and 0.17V vs.Li/Li$^+$respectively. Hence the voltage hysteresis is formed around 1V vs. Li/Li$^+$. The anode composites show parabolic curves at around 0.5 and 0.2V and flat plateaus between 0.1 and 0.0V, which is normal in composite materials. The slopes usually emerge due to the existence of carbon in the composite materials.Table 4.1. shows the theoretical and the calculated specific capacity at each current density.

Table 4.1. Theoretical capacities and calculated specific capacities at different c-rates

		Calculated Specific Capacity / mAh/g				
Samples	**Theoretical Capacity / mAh/g**	**C/10**	**C/5**	**C/2**	**1C**	**2C**
MCMB	372	334	320	255	132	63
5wt% Si	531	496	395	287	199	81
10wt% Si	692	567	430	268	136	58
15wt% Si	853	649	461	331	162	48

4.2.3. Cyclic voltammetry (CV)

The cyclic voltammograms of five cycles for the Si-MCMB compositesare presented in Figure 4.10.

The CV analysis of the produced anodes was carried out in a voltage window of 1.5-0.02V at a 0.3mV/sec scanning rate. The upper and lower half of the curve represents the oxidation and the reduction peaks and correspond to the charging and discharging of the cellrespectively. These peaks also refer to anodic and cathodic peaks. In the anodic reaction (charging state), the potential rises from 0.02-1.5V, where the lithium ions delithiate from the structure of the composite. During this phase, the CV test revealed the anodic peaks at around 0.3 and 0.5V.Inversely, in the cathodic reaction (discharging state), the potential goes back from 1.5-0.02V, where the lithium ions lithiate into the composite structure.

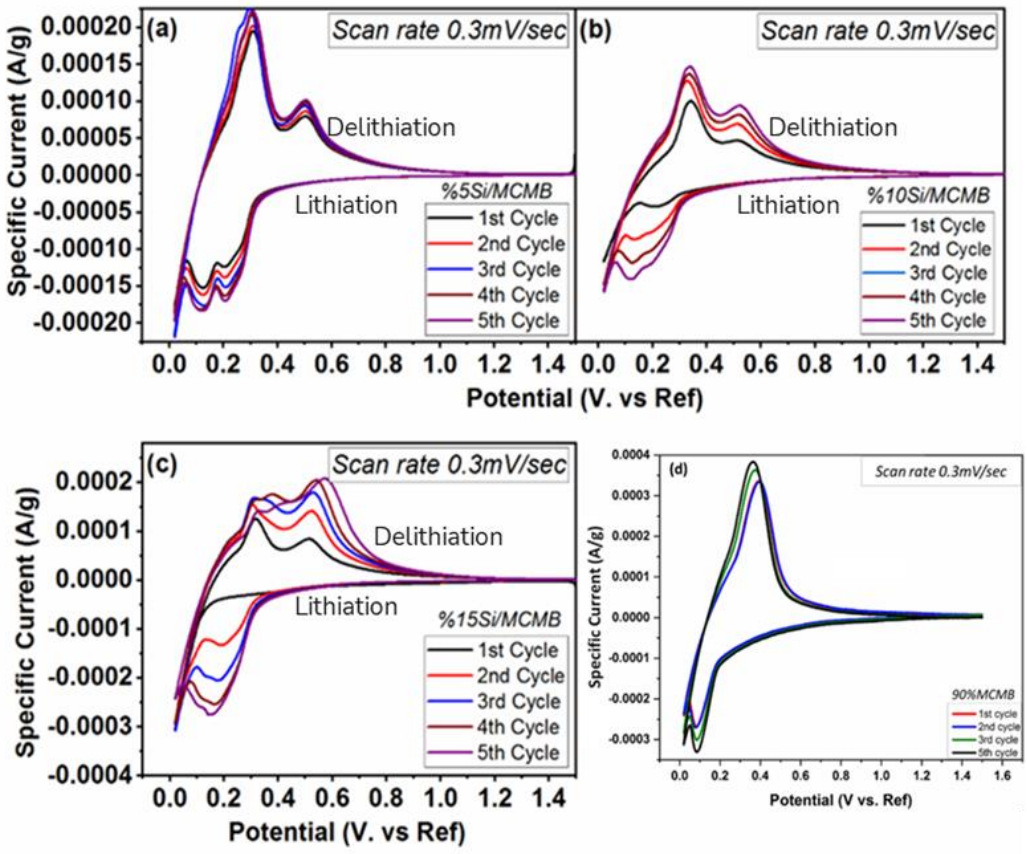

Figure 4.10. Cyclic Voltammograms of 1st to 5th cycle of the composites and MCMB between 1.5-0.02V

The Two cathodic peaks appeared at around 0.1 and 0.25V during this phase, as shown in figures 4.10a.and b. These peaks should attribute to the lithiation and delithiation of Si particles in the MCMB matrix. The anodic peaks for all samples are ascribed to the development of the SEI layer, and the magnitudes of both oxidation and reduction peaks have increased with cycling, indicating the activation of further material to react with lithium, as shown in figure 4.10b., and c. Additionally, the gap between the anodic and cathodic peaks attributes to the polarization of the electrode. The curves in the 5wt% Si-MCMB composite are identical and overlappedwith each other over five cycles, demonstrating the stability of the electrode with cycling.In the 15wt%Si-MCMB sample, the anodic peaks slightly moved from 0.5V to 0.6V, suggesting an increased anode polarization and irreversibility of the material.

4.2.4. Electrochemical impedance spectroscopy (EIS)

To examine the mechanisms for better cycling performance of Si-MCMB composites

and MCMB electrode, impedance tests of both electrodes were compared before and after the electrochemical charge-discharge cycling in an open circuit potential of 2V.

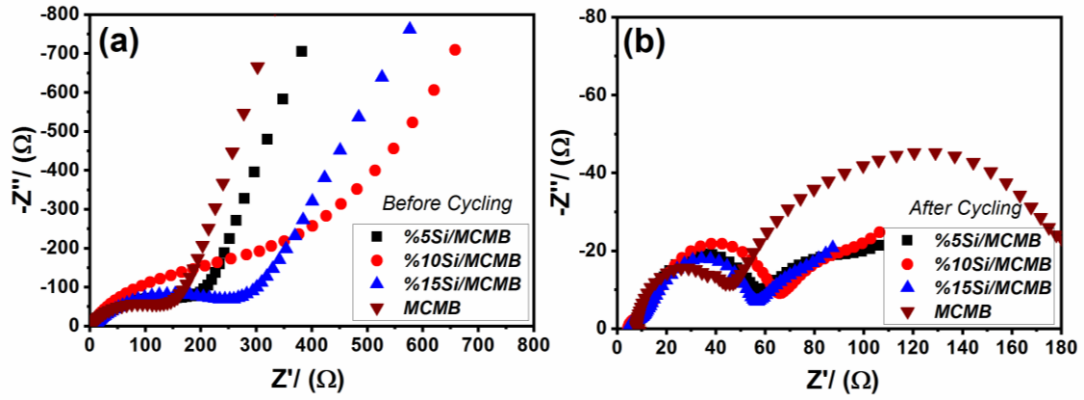

Figure 4.11. Nyquist plots of the composite electrodes and MCMB

Figure 4.11. shows all Nyquist plots comprised of depressed circles in a high-frequency range and inclined lines in a low-frequency range. The compressed semicircles correspond to the R_{ct} on the interface of an anode, and the ionic conductivity of the electrolyte, while the inclined lines with an angle to real axis represent typical Warburg behavior and correspond to the lithium-ion diffusion into the layers of composite anodes. The two semicircles in the MCMB electrode are generated due to the roughness of the electrode surface and its microstructure's porosity and attributed to the non-ideal response of the capacitance [131]. As can be seen, the diameters of the high-frequency semicircles (at about 200Ω) have reduced around 50-60Ω after cycling, indicating that the surface had improved kinetics for charge transfer with cycling, and active sites of the material have been exposed more to the electrolyte.

4.3. State-of-Charge (SOC) Analysis

For the evaluationof the SOC, the rate capability for the new set of composite electrodes was investigated in three different voltage windows, presented in Figure 4.12. The upper cut-off voltage was decreased to 1V for all the samples, while the lower cut-off voltages were applied as 0.03V, 0.05V and 0.07V.In other words, the voltage windows were decreased as whole. The same current densities and the same

number of cycles were set as for the previously cycled anodes, which were tested in a voltage window between 1.5-0.02V.

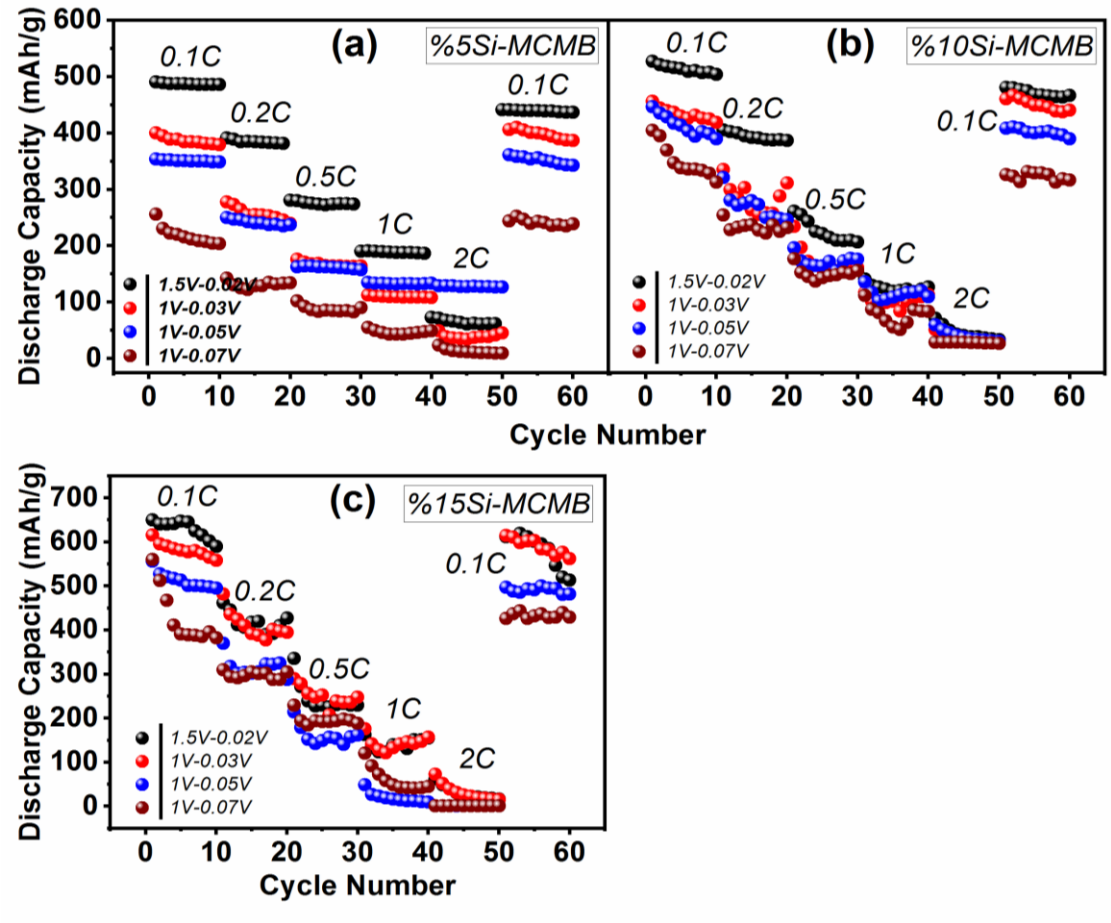

Figure 4.12. Rate performance of composites under different voltage voltages vs. standard volatge window

According to the above rate analysis, it is commendable that by decreasing the upper cut-off voltage (1.5V to 1V)and by increasing the lower cut-off voltage (0.02V to 0.07V), and increasing the c-rates,the stress level increases and accumulates more pressure to destroy the electrode, leading to more capacity loss.Inversely, decreasing trend in the lower cut-off voltagecontributes to slow capacity decay and lower stress level [132]. Interestingly, these electrodes showed the same behavior just like the already cycled electrodes in a standard potential range, where the one with the highest Si content (15wt %) showed unstable performance over 60 cycles. To evaluate an optimum Si content and optimum voltage window, the best

performingelectrode was the one containing the lowest amount of Si (5wt%), where it retained its capacity in a voltage window between 1-0.05V.

Furthermore, Figure 4.13.confirmed that the stress level induced by varyingthe whole voltage window from 1-0.03V to 1-0.07V. In Figure 4.13b., major surface cracks were observedin the composite anode cyled between 1-0.07V.

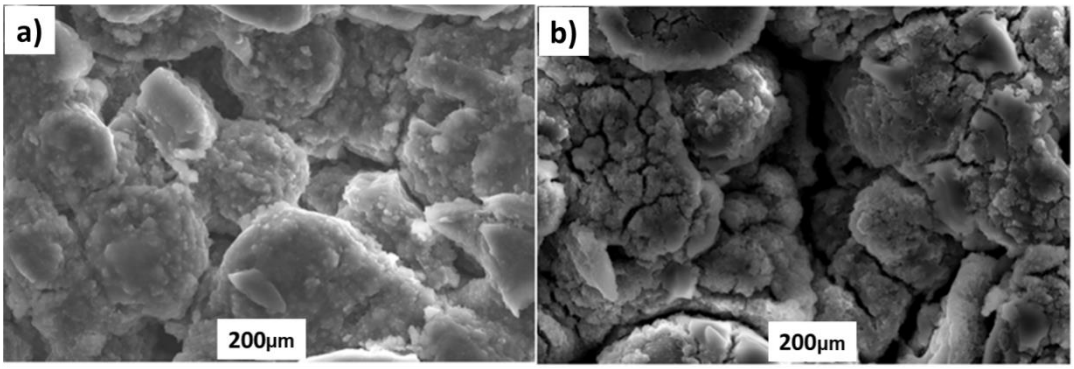

Figure 4.13. SEM images of electrodes after electrochemical tests (a) voltage window between 1-0.03V (b) voltage window between 1-0.07V

For the electrode cycled between 1-0.03V, the electrode has gone through minor surface cracks, as presented in Figure 4.13a. Such results recomend that the small cut-off voltages createmore pressure on the electrode's surface, leading to severe surface cracking and ultimately experience faster capacity loss.

Moreover, from the above evidence, a cut-off voltage window between 1-0.05V was selected for cycle life testing to evaluate their long-term performance. Figure 4.14. shows the cycle life performance of the composite electrodes at c-rates of C/2 and 1C. A total of six samples were assembled for this test, and each cell was tested for 200 cycles. Before starting the electrochemical testing, one formation cycle for all the electrodes was performed at a slow c-rate of C/20 to establish a stable SEI layer. As visible inFigure 4.14. below, the capacity loss is enormous in the initial cycles for all the electrodes because of the formation of the SEI layer and the pulverization of Si particles.This phenomenon can continue for more cycles on the surface of active material if no formation cycling is performed at a slow c-rate [133]. 15wt% Si electrode showed the worst cycling performance compared to the electrodes

containing 5wt% and 10wt% Si amount.From this evidence, it is clear that increasing the Si-C ratio in the composites does not directly enhance the total anode capacity due to the massive volume expansion of Si. The 5wt% composite electrode exhibited the best cycling performance with a stable capacity of 182mAh/g at C/2 and 170mAh/g at 1C over 200 cycles. On the other hand, 10w% Si sample has lost 19% of its capacity at C/2 and 64% at 1C after 200 cycles.

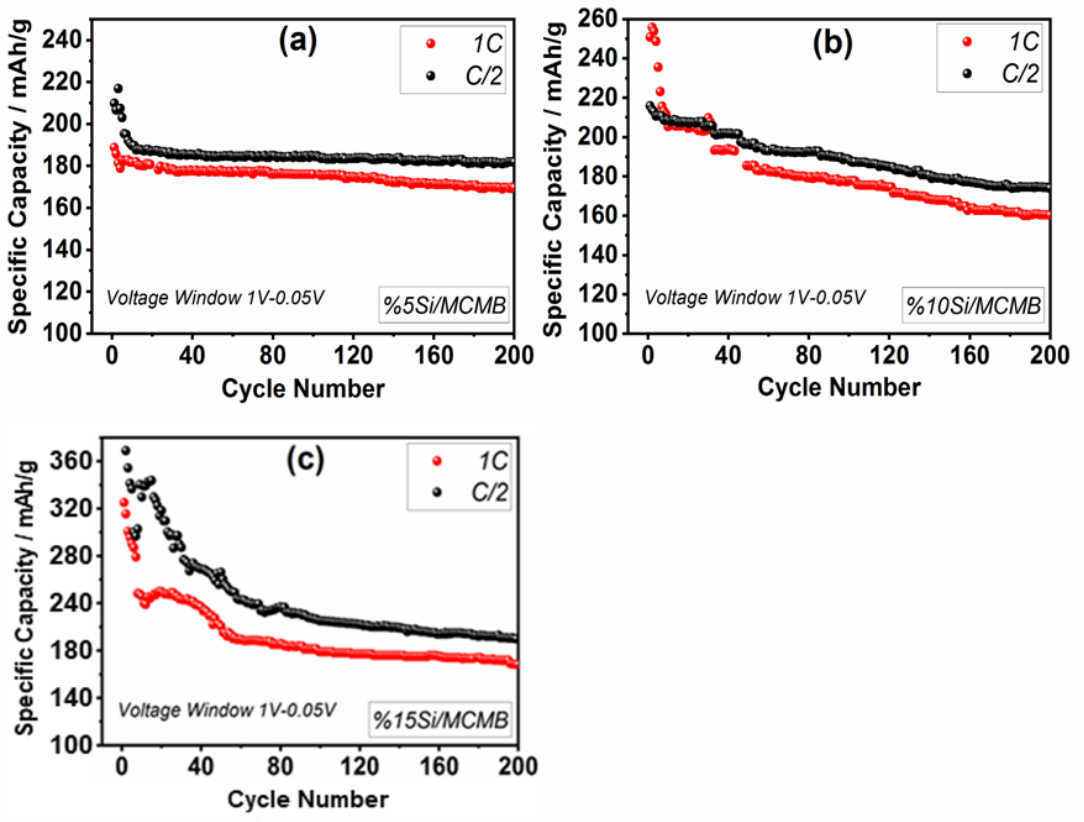

Figure 4.14. Cycling performanceof electrodes cycled under 1-0.05V cut-off voltage at 1C and C/2

Similarly, 15wt% Si electrode has retained 54% capacity at C/2 and 58% capacity at 1C, which is much lower than 87% and 90% capacity retention at C/2 and 1C of the 5wt% Si electrode, respectively.

CHAPTER 5. CONCLUSION

Adjustment of Si with graphite is an encouraging approach to increase the specific capacity of the negative electrodes, which has a theoretical capacity of approximately ten times higher than graphite. In this master thesis, it was proposed to develop a LIB anode with a higher specific capacity. To accomplish this, nano Si powder (<100nm) was commercially purchased. The nano Si powderwasmixed with the MCMB powder in small amounts via mechanical alloying to produce a nanocomposite anode for LIB instead of the bare graphite anode used in commercial LIBs. The percentage of Si was varied to 5wt%, 10wt%, and 15wt% by weight to determine the rate and cycling performance in different conditions. The optimized nanocomposite anodes have been morphologically and electrochemically treated through SEM-EDS imaging and galvanostatic charge-discharge testing, respectively.

In the electrochemical charge-discharge examinations, 5wt% Si retained a stable capacity of 455mAh/g in the rate capability test over 60 cycles compared to 10 wt% and 15 wt% Si content. Our analysis revealed that by increasing the Si content, there is a huge capacity drop and the higher Si content electrodes showed unstable capacitive behavior with consequent cycles, even lower than the specific capacity of pure MCMB electrode. Additionally, during the SOC analysis, 5wt% Si electrode showed capacity retention of 88% and 90% for 200 cycles at c-rates of C/2 and 1C respectively, in the potential range between 1-0.05V.

Lastly, based on the findings of this research, it isconcluded that higher current rates (2C and more) are not feasible for Si-based composite electrodes.

REFERENCES

[1] Tarascon, J. M., Armand, M., Issues and challenges facing rechargeable lithium batteries. Materials for sustainable energy.,414(6861): 171-179, 2011.

[2] Park, O.K.,Cho, Y., Lee, S., Yoo, H. C., Song, H. K., Cho, J., Who will drive electric vehicles, olivine or spinel?. Energy & Environmental Science., 4(5): 1621-1633, 2011.

[3] Arico, A. S., Bruce, P., Scrosati, B., Tarascon, J. M., Van Schalkwijk, W., Nanostructured materials for advanced energy conversion and storage devices. Materials for sustainable energy: a collection of peer-reviewed research and review articles. Nature Publishing Group., 148-159, 2011

[4] Wu, Y., E. Rahm., R. Holze., Carbon anode materials for lithium ion batteries. Journal of power sources., 114(2): 228-236, 2003.

[5] Kasavajjula, U., Wang, C., Appleby, A. J., Nano-and bulk-silicon-based insertion anodes for lithium-ion secondary cells. Journal of power sources., 163(2): 1003-1039, 2007.

[6] Ashuri, M., He, Q., & Shaw, L. L., Silicon as a potential anode material for Li-ion batteries: where size, geometry and structure matter. Nanoscale., 8(1): 74-103, 2016.

[7] Su, X., Wu, Q., Li, J., Xiao, X., Lott, A., Lu, W., Wu, J.,Silicon-based nanomaterials for lithium-ion batteries: a review. Advanced Energy Materials., 4(1): 1300882, 2014.

[8] Szczech, J. R.,Jin, S., Nanostructured silicon for high capacity lithium battery anodes. Energy & Environmental Science., 4(1): 56-72, 2011.

[9] Palomares, V., Serras, P., Villaluenga, I., Hueso, K. B., Carretero-González, J., Rojo, T., Na-ion batteries, recent advances and present challenges to become low cost energy storage systems. Energy & Environmental Science., 5(3): 5884-5901, 2012.

[10] Yoshio, M., Brodd, R. J., Kozawa, A., Lithium-Ion Batteries. Springer, 1stEdition, 2009.

[11] Skundin, A. M., Efimov, O. N., Ol'ga, V. Y., The state-of-the-art and prospects for the development of rechargeable lithium batteries. Russian chemical reviews., 71(4): 329-346, 2002.

[12] Ohzuku, T., Brodd, R. J., An overview of positive-electrode materials for advanced lithium-ion batteries. Journal of Power Sources., 174(2): 449-456, 2007.

[13] Scrosati, B., Garche, J., Lithium batteries: Status, prospects and future. Journal of power sources., 195(9): 2419-2430, 2010.

[14] Besenhard, J. O., Handbook of battery materials. John Wiley & Sons, 2nd Edition, 2008.

[15] Winter, M., Brodd., R. J., What are batteries, fuel cells, and supercapacitors?. Chemical reviews., 104(10): 4245-4270, 2004.

[16] Linden, D., Reddy, T. B., Handbook of Batteries. McGraw Hill, 3rd edition, 1995.

[17] Teki, R., Datta, M. K., Krishnan, R., Parker, T. C., Lu, T. M., Kumta, P. N., Koratkar, N., Nanostructured silicon anodes for lithium ion rechargeable batteries., 5(20): 2236-2242, 2009.

[18] Touzain, P., Yazami, R., Maire, J., U.S. Patent No. 4,584,252. Washington, DC: U.S. Patent and Trademark Office, 1986.

[19] Chen, J., Law, C. C., Lam, J. W., Dong, Y., Lo, S. M., Williams, I. D., Tang, B. Z., Synthesis, light emission, nanoaggregation, and restricted intramolecular rotation of 1, 1-substituted 2, 3, 4, 5-tetraphenylsiloles. Chemistry of materials, 15(7):1535-1546, 2003.

[20] Thackeray, M. M., Wolverton, C., & Isaacs, E. D., Electrical energy storage for transportation—approaching the limits and going beyond lithium-ion batteries., Energy & Environmental Science, 5(7): 7854-7863, 2012.

[21] Aifantis, K. E., Hackney, S. A., Kumar, R. V.,High energy density lithium batteries: Materials, Engineering, Applications. Wiley VCH, 2010.

[22] Ehrlich, G. M., Lithium-ion batteries. Handbook of batteries, McGraw-Hill New York, NY, USA 3, 2002.

[23] Sun, Y., Shiosaki, Y., Xia, Y., Noguchi, H., The preparation and electrochemical performance of solid solutions LiCoO2–Li2MnO3 as cathode materials for lithium ion batteries. Journal of power sources, 159(2): 1353-1359, 2006.

[24] Andersen, H. F, (2014). New Materials for Lithium-Ion Batteries. Bayerische Julius-Maximilians-Universitaet Wuerzburg (Germany)

[25] Zhang, Z. J., Ramadass, P.,Lithium-ion battery systems and technology. In Batteries for Sustainability (pp. 319-357). Springer, New York, NY, 2013.

[26] Luo, W., Chen, X., Xia, Y., Chen, M., Wang, L., Wang, Q., Yang, J., Surface and interface engineering of silicon-based anode materials for lithium-ion batteries. Advanced Energy Materials, 7(24): 1701083, 2017.

[27] Li, H., Wang, Z., Chen, L., Huang, X., Research on advanced materials for Li-ion batteries. Advanced materials, 21(45): 4593-4607, 2009.

[28] Sides, C. R., Martin, C. R., Nanostructured electrodes and the low-temperature performance of Li-ion batteries. Advanced Materials, 17(1): 125-128, 2005.

[29] Xu, Kang., Electrolytes and interphasial chemistry in Li ion devices. Energies, 3(1): 135-154, 2010.

[30] Ji, L., Lin, Z., Alcoutlabi, M., Zhang, X., (2011). Recent developments in nanostructured anode materials for rechargeable lithium-ion batteries. Energy & Environmental Science, 4(8): 2682-2699. 2011.

[31] Kim, T., Song, W., Son, D. Y., Ono, L. K., Qi, Y., Lithium-ion batteries: outlook on present, future, and hybridized technologies. Journal of materials chemistry, 7(7): 2942-2964, 2019.

[32] Guo, P., Song, H., Chen, X., Electrochemical performance of graphene nanosheets as anode material for lithium-ion batteries. Electrochemistry Communications, 11(6): 1320-1324, 2009.

[33] Dahn, J. R., Zheng, T., Liu, Y., Xue, J. S., Mechanisms for lithium insertion in carbonaceous materials. Science, 270(5236): 590-593, 1995.

[34] Li, H., Wang, Z., Chen, L., Huang, X., Research on advanced materials for Li-ion batteries. Advanced materials, 21(45): 4593-4607, 2009.

[35] Zhang, W. J., A review of the electrochemical performance of alloy anodes for lithium-ion batteries. Journal of Power Sources, 196(1): 13-24, 2011.

[36] Chen, X., Du, Y., Zhang, N. Q., Sun, K. N., 3D self-supported nanoarchitectured arrays electrodes for lithium-ion batteries. Journal of Nanomaterials, 2012, 2012.

[37] Deng, D., Kim, M. G., Lee, J. Y., Cho, J., Green energy storage materials: Nanostructured TiO2 and Sn-based anodes for lithium-ion batteries. Energy & Environmental Science, 2(8): 818-837, 2009.

[38] Ellis, B. L., Lee, K. T., Nazar, L. F., Positive electrode materials for Li-ion and Li-batteries. Chemistry of materials, 22(3): 691-714, 2010.

[39] Whittingham, M. S., Lithium batteries and cathode materials. Chemical reviews, 104(10): 4271-4302, 2004.

[40] Wang, Y., Cao, G., Developments in nanostructured cathode materials for high-performance lithium-ion batteries. Advanced materials, 20(12): 2251-2269, 2008.

[41] Needham, S. A., Wang, G. X., Liu, H. K., Drozd, V. A., Liu, R. S., Synthesis and electrochemical performance of doped LiCoO2 materials. Journal of Power Sources, 174(2): 828-831, 2007.

[42] Liu, H., Wu, Y. P., Rahm, E., Holze, R., Wu, H. Q., Cathode materials for lithium ion batteries prepared by sol-gel methods. Journal of Solid State Electrochemistry, 8(7): 450-466, 2004.

[43] Fergus, J. W., Recent developments in cathode materials for lithium ion batteries. Journal of power sources, 195(4): 939-954, 2010.

[44] Park, S. I., Okada, S., Yamaki, J. I., Symmetric Cell with LiMn_2O_4 for Aqueous Lithium-ion Battery. Journal of novel carbon resource sciences, 3: 27-31, 2011.

[45] Bao, S. J., Liang, Y. Y., Li, H. L., Synthesis and electrochemical properties of LiMn2O4 by microwave-assisted sol–gel method. Materials Letters, 59(28): 3761-3765, 2005.

[46] Zhong, Q., Bonakdarpour, A., Zhang, M., Gao, Y., Dahn, J. R., Synthesis and Electrochemistry of LiNixMn2−xO4. Journal of the Electrochemical Society, 144(1): 205, 1997.

[47] Rossen, E., Jones, C. D. W., Dahn, J. R., Structure and electrochemistry of LixMnyNi1− yO2. Solid State Ionics, 57(3-4): 311-318, 1992.

[48] Spahr, M. E., Novák, P., Schnyder, B., Haas, O., Nesper, R., Characterization of layered lithium nickel manganese oxides synthesized by a novel oxidative coprecipitation method and their electrochemical performance as lithium insertion electrode materials, Journal of the electrochemical Society, 145(4): 1113, 1998.

[49] Armstrong, A. R., Bruce, P. G., Synthesis of layered LiMnO2 as an electrode for rechargeable lithium batteries. Nature, 381(6582): 499-500, 1996.

[50] Julien, C., Mauger, A., Vijh, A., Zaghib, K. (2016). Lithium batteries. In Lithium batteries, 29-68). Springer, Cham.

[51] Profatilova, I. A., Langer, T., Badillo, J. P., Schmitz, A., Orthner, H., Wiggers, H., Winter, M.,Thermally induced reactions between lithiated nano-silicon electrode and electrolyte for lithium-ion batteries. Journal of the electrochemical Society, 159(5): A657, 2012.

[52] Nakai, H., Kubota, T., Kita, A., Kawashima, A.,Investigation of the solid electrolyte interphase formed by fluoroethylene carbonate on Si electrodes. Journal of the Electrochemical Society, 158(7): A798, 2011.

[53] Ulldemolins, M., Le Cras, F., Pecquenard, B., Phan, V. P., Martin, L., Martinez, H., Investigation on the part played by the solid electrolyte interphase on the electrochemical performances of the silicon electrode for lithium-ion batteries. Journal of Power Sources, 206: 245-252, 2012.

[54] Lindgren, F., Xu, C., Niedzicki, L., Marcinek, M., Gustafsson, T., Björefors, F., Younesi, R., SEI formation and interfacial stability of a Si electrode in a LiTDI-salt based electrolyte with FEC and VC additives for Li-ion batteries. ACS applied materials & interfaces, 8(24): 15758-15766, 2016.

[55] Arora, P., Zhang, Z., Battery separators. Chemical reviews, 104(10): 4419-4462, 2004.

[56] Myung, S. T., Hitoshi, Y., Sun, Y. K., Electrochemical behavior and passivation of current collectors in lithium-ion batteries. Journal of Materials Chemistry, 21(27): 9891-9911, 2011.

[57] Oltean G. From Current Collectors to Electrodes: Aluminium Rod Structures for Three-dimensional Li-ion Micro-battery Applications. Acta Universitatis Upsaliensis, 2014.

[58] Liang, B., Liu, Y., Xu, Y., Silicon-based materials as high capacity anodes for next generation lithium ion batteries. Journal of Power sources, 267: 469-490, 2014.

[59] Casimir, A., Zhang, H., Ogoke, O., Amine, J. C., Lu, J., Wu, G., Silicon-based anodes for lithium-ion batteries: Effectiveness of materials synthesis and electrode preparation. Nano Energy, 27: 359-376, 2016.

[60] Beattie, S. D., Larcher, D., Morcrette, M., Simon, B., Tarascon, J. M., Si electrodes for Li-ion batteries—a new way to look at an old problem. Journal of the Electrochemical Society, 155(2): A158, 2007.

[61] Beattie, S. D., Larcher, D., Morcrette, M., Simon, B., Tarascon, J. M., Si electrodes for Li-ion batteries—a new way to look at an old problem. Journal of The Electrochemical Society., 155(2): A158, 2007

[62] Terranova, M. L., Orlanducci, S., Tamburri, E., Guglielmotti, V., Rossi, M., Si/C hybrid nanostructures for Li-ion anodes: An overview. Journal of Power Sources., 246 (1): 167-177, 2004.

[63] Klett, M., Gilbert, J. A., Pupek, K. Z., Trask, S. E., Abraham, D. P., Layered oxide, graphite and silicon-graphite electrodes for lithium-ion cells: effect of electrolyte composition and cycling windows. Journal of The Electrochemical Society., 164(1): A6095, 2016.

[64] Peled, E., Menkin, S., SEI: past, present and future. Journal of The Electrochemical Society., 164(7): A1703, 2017.

[66] Jung, R., Metzger, M., Haering, D., Solchenbach, S., Marino, C., Tsiouvaras, N., Gasteiger, H. A., Consumption of fluoroethylene carbonate (FEC) on Si-C composite electrodes for Li-ion batteries. Journal of The Electrochemical Society., 163(8): A1705, 2016.

[66] Mukerjee, AK., Dasgupta, N., DC power supply used as photovoltaic simulator for testing MPPT algorithms. Renew Energy., 32(4): 587–592, 2007.

[67] Nitta, N., Wu, F., Lee, J. T.,Yushin, G., Li-ion battery materials: present and future. Materials today., 18(5): 252-264, 2015.

[68] Anani, A., Huggins, R. A., Multinary alloy electrodes for solid state batteries II. A new Li SiMg alloy negative electrode material for use in high energy density rechargeable lithium cells. Journal of power sources., 38(3): 363-372, 1992.

[69] Hashimoto, Y., Machida, N., Shigematsu, T., Preparation of Li4. 4GexSi1− x alloys by mechanical milling process and their properties as anode materials in all-solid-state lithium batteries. Solid State Ionics,. 175(1-4): 177-180, 2004.

[70] Schäfer, H., Axel, H., Weiss, A., Neue Phasenim System Lithium—Silicium. Zeitschrift für Naturforschung B., 20(12): 1302-1302, 1965.

[71] Axel, H., Schäfer, H.,Weiss, A., Zur kenntnis der phase Li22Si5. Zeitschrift für Naturforschung B., 21(2): 115-117, 1966.

[72] Seefurth, R. N., Sharma, R. A., Investigation of lithium utilization from a lithium-silicon electrode. Journal of The Electrochemical Society., 124(8): 1207, 1977.

[73] Kasavajjula, U., Wang, C., Appleby, A. J., Nano-and bulk-silicon-based insertion anodes for lithium-ion secondary cells. Journal of power sources., 163(2): 1003-1039, 2007.

[74] Zhang, W. J., A review of the electrochemical performance of alloy anodes for lithium-ion batteries. Journal of Power Sources., 196(1): 13-24, 2011.

[75] McDowell, M. T., Lee, S. W., Nix, W. D., Cui, Y., 25th anniversary article: understanding the lithiation of silicon and other alloying anodes for lithium-ion batteries. Advanced Materials., 25(36): 4966-4985, 2013.

[76] Thackeray, M. M., Wolverton, C.,Isaacs, E. D., Electrical energy storage for transportation—approaching the limits of, and going beyond, lithium-ion batteries. Energy & Environmental Science., 5(7): 7854-7863, 2012.

[77] Yoshio, M., Wang, H., Fukuda, K., Umeno, T., Dimov, N., Ogumi, Z., Carbon-coated Si as a lithium-ion battery anode material. Journal of The Electrochemical Society., 149(12): A1598, 2002.

[78] Boukamp, B. A., Lesh, G. C., Huggins, R. A., All-solid lithium electrodes with mixed-conductor matrix. Journal of the Electrochemical Society., 128(4): 725, 1981.

[79] He, Y., Yu, X., Wang, Y., Li, H., Huang, X., Alumina-coated patterned amorphous silicon as the anode for a lithium-ion battery with high Coulombic efficiency. Advanced materials., 23(42): 4938-4941, 2011.

[80] Rehnlund, D., Lindgren, F., Böhme, S., Nordh, T., Zou, Y., Pettersson, J.,Nyholm, L., Lithium trapping in alloy forming electrodes and current collectors for lithium based batteries. Energy & Environmental Science., 10(6): 1350-1357, 2017.

[81] Wu, H., Cui, Y., Designing nanostructured Si anodes for high energy lithium ion batteries. Nano today., 7(5): 414-429, 2012.

[82] Obrovac, M. N., Christensen, L., Structural changes in silicon anodes during lithium insertion/extraction. Electrochemical and solid-state letters,. *7*(5): A93, 2004.

[83] Gómez-Cámer, J. L., Bünzli, C., Hantel, M. M., Poux, T.,Novák, P., On the correlation between electrode expansion and cycling stability of graphite/Si electrodes for Li-ion batteries. Carbon., 105 (1): 42-51, 2016.

[84] Nitta, N., Yushin, G., High-capacity anode materials for lithium-ion batteries: choice of elements and structures for active particles. Particle & Particle Systems Characterization., 31(3): 317-336, 2014.

[85] Hovington, P., Dontigny, M., Guerfi, A., Trottier, J., Lagacé, M., Mauger, A., Zaghib, K., In situ Scanning electron microscope study and microstructural evolution of nano silicon anode for high energy Li-ion batteries. Journal of Power Sources., 248, 457-464, 2014.

[86] Liu, D., Liu, Z. J., Li, X., Xie, W., Wang, Q., Liu, Q., He, D., Group IVA element (Si, Ge, Sn)-based alloying/dealloying anodes as negative electrodes for full-cell lithium-ion batteries. Small., 13(45): 1702000, 2017.

[87] Park, M. S., Wang, G. X., Kang, Y. M., Wexler, D., Dou, S. X., Liu, H. K., Preparation and electrochemical properties of SnO2 nanowires for application in lithium-ion batteries. Angewandte Chemie International Edition., 46(5): 750-753, 2007.

[88] Shi, S. L., Liu, Y. G., Zhang, J. Y., Wang, T. H., CROSS-DISCIPLINARY PHYSICS AND RELATED AREAS OF SCIENCE AND TECHNOLOGY: Electrochemical properties of SnO2 nanorods as anode materials in lithium-ion battery. Chinese Physics B., 18(10): 4564-4570, 2009.

[89] Vetter, J., Novák, P., Wagner, M. R., Veit, C., Möller, K. C., Besenhard, J. O.,Hammouche, A., Ageing mechanisms in lithium-ion batteries. Journal of power sources., 147(1-2): 269-281, 2005.

[90] Joho, F., Novák, P., Spahr, M. E., Safety aspects of graphite negative electrode materials for lithium-ion batteries. Journal of the Electrochemical Society., 149(8): A1020, 2002.

[91] Erdinc, O., Vural, B., Uzunoglu, M., A dynamic lithium-ion battery model considering the effects of temperature and capacity fading. International Conference on Clean Electrical Power, 383-386, 2009.

[92] G. Sarre, P. Blanchard, M. Broussely, Journal of Power Sources 127 (1-2)(2004) 65-71. Eighth Ulmer Electrochemische Tage.

[93] A. Ritchie, Journal of Power Sources 136 (2) (2004) 285e289. Selected Papers Presented at the International Power Sources Symposium

[94] W. Bögel, J.P. Büchel, H. Katz, Journal of Power Sources 72 (1) (1998) 37-42.

[95] Bloom, I., Cole, B. W., Sohn, J. J., Jones, S. A., Polzin, E. G., Battaglia, V. S., Case, H. L.,An accelerated calendar and cycle life study of Li-ion cells. Journal of power sources, 101(2): 238-247., 2001

[96] Wright, R. B., Motloch, C. G., Belt, J. R., Christophersen, J. P., Ho, C. D., Richardson, R. A., Sutula, R. A.,Calendar-and cycle-life studies of advanced technology development program generation 1 lithium-ion batteries. Journal of power sources, 110(2): 445-470, 2002.

[97] Zhang, S. S., Xu, K., Jow, T. R., Electrochemical impedance study on the low temperature of Li-ion batteries. Electrochimica acta, 49(7): 1057-1061, 2004.

[98] Ohue, K., Utsunomiya, T., Hatozaki, O., Yoshimoto, N., Egashira, M., Morita, M.,Self-discharge behavior of polyacenic semiconductor and graphite negative electrodes for lithium-ion batteries. Journal of power sources, 196(7): 3604-3610, 2011.

[99] Kassem, M., Bernard, J., Revel, R., Pelissier, S., Duclaud, F., Delacourt, C., Calendar aging of a graphite/LiFePO4 cell. Journal of Power Sources, 208, 296-305, 2012.

[100] Barré, A., Deguilhem, B., Grolleau, S., Gérard, M., Suard, F., Riu, D., A review on lithium-ion battery ageing mechanisms and estimations for automotive applications. Journal of Power Sources., 241: 680-689. 2014.

[101] Yang, H., Bang, H., Amine, K., Prakash, J., Batteries, Fuel Cells, and Energy Conversion-Investigations of the Exothermic Reactions of Natural Graphite Anode for Li-Ion Batteries during Thermal Runaway. Journal of the Electrochemical Society., 152(1): A73, 2005.

[102] Nunotani, K., Yoshida, F., Kamiya, Y., Daisho, Y., Abe, K., Kono, M., Matsuo, H., Development and performance evaluation of lithium iron phosphate battery with superior rapid charging performance—Second report: Evaluation of battery capacity loss characteristics. IEEE Vehicle Power and Propulsion Conference., 1-4, 2011.

[103] Liu, P., Wang, J., Hicks-Garner, J., Sherman, E., Soukiazian, S., Verbrugge, M., Finamore, P., Aging mechanisms of LiFePO4 batteries deduced by electrochemical and structural analyses. Journal of the Electrochemical Society., 157(4): A499, 2010.

[104] Kötz, R., Ruch, P. W., Cericola, D., Aging and failure mode of electrochemical double layer capacitors during accelerated constant load tests. Journal of power sources., 195(3): 923-928, 2010.

[105] Wu, Y. P., Rahm, E., Holze, R., Carbon anode materials for lithium ion batteries. Journal of power sources., 114(2): 228-236, 2003.

[106] Buqa, H., Würsig, A., Vetter, J., Spahr, M. E., Krumeich, F., Novák, P., SEI film formation on highly crystalline graphitic materials in lithium-ion batteries. Journal of power sources., 153(2): 385-390, 2006.

[107] Zhang, S., Ding, M. S., Xu, K., Allen, J., Jow, T. R., Understanding solid electrolyte interface film formation on graphite electrodes. Electrochemical and Solid-State Letters, 4(12): A206, 2001.

[108] Goers, D., Spahr, M. E., Leone, A., Märkle, W., Novák, P., The influence of the local current density on the electrochemical exfoliation of graphite in lithium-ion battery negative electrodes. Electrochimica Acta., 56(11): 3799-3808, 2011.

[109] Broussely, M. I. C. H. E. L., Herreyre, S., Biensan, P., Kasztejna, P., Nechev, K., Staniewicz, R. J., Aging mechanism in Li ion cells and calendar life predictions. Journal of Power Sources., 97 (1): 13-21, 2001.

[110] Abe, T., Fukuda, H., Iriyama, Y., Ogumi, Z., Solvated Li-ion transfer at interface between graphite and electrolyte. Journal of the Electrochemical Society., 151(8): A1120, 2004.

[111] Chung, G. C., Kim, H. J., Yu, S. I., Jun, S. H., Choi, J. W., Kim, M. H., Origin of graphite exfoliation an investigation of the important role of solvent cointercalation. Journal of The Electrochemical Society., 147(12): 4391, 2000.

[112] Bashash, S., Moura, S. J., Forman, J. C., Fathy, H. K., Plug-in hybrid electric vehicle charge pattern optimization for energy cost and battery longevity. Journal of power sources., 196 (1): 541-549, 2011.

[113] Methekar, R. N., Northrop, P. W., Chen, K., Braatz, R. D., Subramaniana, V. R., PROOF COPY [JES-10-1220R1] 036104JES. Journal of the Electrochemical Society., 158(4): 1-8, 2011.

[114] Koltypin, M., Aurbach, D., Nazar, L., Ellis, B., More on the performance of LiFePO4 electrodes—The effect of synthesis route, solution composition, aging, and temperature. Journal of Power Sources., 174(2): 1241-1250, 2007.

[115] Barré, A., Deguilhem, B., Grolleau, S., Gérard, M., Suard, F., Riu, D., A review on lithium-ion battery ageing mechanisms and estimations for automotive applications. Journal of Power Sources., 241 (1): 680-689, 2013.

[116] Ellis, B. L., Lee, K. T., Nazar, L. F., Positive electrode materials for Li-ion and Li-batteries. Chemistry of materials., 22(3): 691-714, 2010.

[117] Eshetu, G. G., Diemant, T., Hekmatfar, M., Grugeon, S., Behm, R. J., Laruelle, S., Passerini, S., Impact of the electrolyte salt anion on the solid electrolyte interphase formation in sodium ion batteries. Nano Energy., 55, 327-340, 2019.

[118] Kerlau, M., Marcinek, M., Srinivasan, V., Kostecki, R. M., Reprint of “Studies of local degradation phenomena in composite cathodes for lithium-ion batteries”. Electrochimica Acta, 53(3): 1385-1392, 2007.

[119] Amine, K., Liu, J., Belharouak, I., High-temperature storage and cycling of C-LiFePO4/graphite Li-ion cells. Electrochemistry communications, 7(7): 669-673, 2005.

[120] Wohlfahrt-Mehrens, M., Vogler, C., Garche, J., Aging mechanisms of lithium cathode materials. Journal of power sources., 127(1-2): 58-64, 2004.

[121] Thounthong, P., Chunkag, V., Sethakul, P., Sikkabut, S., Pierfederici, S., Davat, B., Energy management of fuel cell/solar cell/supercapacitor hybrid power source. J Power Sources., 196(1): 313–324, 2011.

[122] Ayache, J., Beaunier, L., Boumendil, J., Ehret, G., Laub, D., Sample preparation handbook for transmission electron microscopy: techniques Springer Science & Business Media., 2010.

[123] Nguyen, B. P. N., Chazelle, S., Cerbelaud, M., Porcher, W., Lestriez, B., Manufacturing of industry-relevant silicon negative composite electrodes for lithium ion-cells. Journal of Power Sources., 262: 112-122, 2014.

[124] Ko, M., Chae, S., Ma, J., Kim, N., Lee, H. W., Cui, Y., Cho, J., Scalable synthesis of silicon-nanolayer-embedded graphite for high-energy lithium-ion batteries. Nature Energy., 1(9): 1-8, 2016

[125] Chen, M., Li, B., Liu, X., Zhou, L., Yao, L., Zai, J.,Yu, X., Boron-doped porous Si anode materials with high initial coulombic efficiency and long cycling stability. Journal of Materials Chemistry A., 6(7): 3022-3027, 2018.

[126] Bindumadhavan, K., Srivastava, S., Srivastava, I., Green synthesis of graphene. J. Nanosci. Nanotechnol., 13(6): 4320-4324, 2013.

[127] Nordh, T., Jeschull, F., Younesi, R., Koçak, T., Tengstedt, C., Edström, K., Brandell, D., Different shades of Li4Ti5O12 composites: The impact of the binder on interface layer formation. ChemElectroChem., 4(10): 2683-2692, 2017.

[128] Jeschull, F., Brandell, D., Wohlfahrt-Mehrens, M., Memm, M., Water-soluble binders for lithium-ion battery graphite electrodes: slurry rheology, coating adhesion, and electrochemical performance. Energy Technology., 5(11): 2108-2118, 2017.

[129] Domi, Y., Usui, H., Iwanari, D., Sakaguchi, H., Effect of mechanical pre-lithiation on electrochemical performance of silicon negative electrode for lithium-ion batteries. Journal of The Electrochemical Society., 164(7): A1651, 2017.

[130] Julien, C., Mauger, A., Vijh, A., Zaghib, K., Electrolytes and Separators for Lithium Batteries. Lithium BatteriesSpringer., 431-460, 2016.

[131] Ahmad, S., Ahmad, M., Mehta, B. R., Gupta, A., Effect of nano-fillers on capacity retention and rate capability of mesocarbon microbeads anode. Journal of The Electrochemical Society., 16413): A2967, 2017.

[132] Zhang, K., Zhang, Y., Zhou, J., Li, Y., Zheng, B., Yang, F., Kai, Y. , A stress-based charging protocol for silicon anode in lithium-ion battery: Theoretical and experimental studies. Journal of Energy Storage., 32(1): 101765, 2020.

[133] Holtstiege, F., Bärmann, P., Nölle, R., Winter, M., Placke, T., Pre-lithiation strategies for rechargeable energy storage technologies: Concepts, promises and challenges. Batteries., 4(1): 4, 2018.

RESUME

Name Surname **:** Salman AHMAD

EDUCATION

Degree	School	Graduation Year
Master's	Sakarya University/ Institute of Natural Sciences / Nanoscience and Nanengineering	Continue
Undergarduate	University of Engineering and Technology Peshawar/ Department of Electronics Engineering	2014
High School	Govt. Degree College	2007

WORK EXPERIENCE

Year	Place	Position
2020-Present	Sakarya University	Researcher

FOREIGN LANGUAGES

English Advance level
Turkish Lower internediate level

HOBBIES

Travelling, Music, Sports